

**Quantitation of Spatially-Localized Protein in Tissue Samples using MALDI-MRM
Imaging**

by

Elizabeth J. Clemis
BSc, University of Victoria, 2008

A Thesis Submitted in Partial Fulfillment
of the Requirements for the Degree of

MASTER OF SCIENCE

in the Department of Biochemistry and Microbiology

© Elizabeth J. Clemis, 2012
University of Victoria

All rights reserved. This thesis may not be reproduced in whole or in part, by photocopy
or other means, without the permission of the author.

Supervisory Committee

Quantitation of Spatially-Localized Protein in Tissue Samples using MALDI-MRM Imaging

by

Elizabeth J. Clemis
BSc, University of Victoria, 2008

Supervisory Committee

Christoph H. Borchers, Department of Biochemistry and Microbiology
Supervisor

Robert Burke, Department of Biochemistry and Microbiology
Departmental Member

Scott McIndoe, Department of Chemistry
Outside Member

Pierre Chaurand, Department of Chemistry (University of Montreal)
Additional Member

Abstract

Supervisory Committee

Christoph H. Borchers, Department of Biochemistry and Microbiology

Supervisor

Robert Burke, Department of Biochemistry and Microbiology

Departmental Member

Scott McIndoe, Department of Chemistry

Outside Member

Pierre Chaurand, Department of Chemistry (University of Montreal)

Additional Member

MALDI imaging allows the creation of a molecular image of a tissue slice. This image is reconstructed from the ion abundances in spectra that are obtained while rastering the laser over the tissue. These images can then be correlated with tissue histology to detect potential biomarkers of, for example, aberrant cell types. MALDI is known to have problems with ion suppression, making it difficult to correlate measured ion abundance with concentration. It would be advantageous to have a method that can provide more accurate protein concentration measurements, particularly for screening applications or for precise comparisons between samples.

My hypothesis was that a method based on multiple reaction monitoring (MRM) with isotopically-labelled internal standards can be developed which would allow the accurate quantitation of proteins in MALDI Imaging. This study reports on the development of this novel MALDI Imaging method for the localization and accurate quantitation of proteins in tissues. This method involves optimization of *in-situ* tryptic digestion, followed by reproducible and uniform deposition of an isotopically-labelled standard peptide from a target protein onto the tissue, using an aerosol-generating device. Data is acquired by MALDI-MRM-MS and accurate peptide quantitation is determined from the ratio of MRM transitions for the endogenous unlabelled proteolytic peptides to the

corresponding transitions from the applied isotopically-labelled standard peptides. In a parallel experiment, the quantity of the labelled peptide applied to the tissue was determined using a standard curve generated from MALDI-TOF-MS data. This external calibration curve was then used to extrapolate the quantity of endogenous peptide in a given area. All standard curves generated by this method had coefficients of determination greater than 0.97. These proof-of-concept experiments using MALDI MRM-based imaging show the feasibility of obtaining precise and accurate quantitation of tissue protein concentrations over two orders of magnitude, while maintaining the spatial localization information for the proteins.

Table of Contents

SUPERVISORY COMMITTEE	II
ABSTRACT	III
TABLE OF CONTENTS.....	V
LIST OF TABLES	VII
LIST OF FIGURES	VIII
LIST OF ABBREVIATIONS.....	IX
ACKNOWLEDGMENTS	X
CHAPTER 1 - INTRODUCTION.....	1
MATRIX ASSISTED LASER DESORPTION IONIZATION.....	1
MALDI TIME-OF-FLIGHT MASS SPECTROMETRY.....	2
<i>Principles of TOF analyzers.....</i>	<i>2</i>
<i>Linear, Reflector and MS/MS mode</i>	<i>3</i>
<i>Detector</i>	<i>5</i>
<i>Bruker Ultraflex III ion source.....</i>	<i>6</i>
TRIPLE QUADRUPOLE MASS SPECTROMETER	6
<i>Principles of MALDI triple quadrupole analyzers</i>	<i>6</i>
<i>MS/MS and MRM</i>	<i>7</i>
<i>The Applied Biosystems MALDI QTRAP 4000</i>	<i>8</i>
<i>Detector</i>	<i>9</i>
MASS SPECTROMETRY-BASED TISSUE IMAGING METHODS	10
MALDI IMAGING.....	11
ADVANTAGES AND LIMITATIONS OF MALDI IMAGING	13
BRUKER IMAGEPREP STATION	16
QUANTITATIVE MALDI IMAGING	17
CHAPTER 2 - PROTEIN CHARACTERIZATION AND SYNTHESIS OF A REPRESENTATIVE PEPTIDE.....	20
INTRODUCTION	20
MATERIALS AND METHODS.....	23
<i>Protein Image.....</i>	<i>23</i>
<i>Peptide Image.....</i>	<i>23</i>
<i>Peptide Identification</i>	<i>24</i>
<i>Synthesis of Light (L) and Heavy (H) Peptides</i>	<i>25</i>
<i>Test for Ion Suppression.....</i>	<i>26</i>
RESULTS.....	28
DISCUSSION.....	32
CHAPTER 3 - QUANTITATION OF THE NORMALIZATION PEPTIDE.	35
INTRODUCTION	35
MATERIALS AND METHODS.....	36
<i>Optimization of peptide deposition method.....</i>	<i>36</i>
<i>Reproducibility of the aerosol deposition method.....</i>	<i>36</i>
<i>MRM normalization</i>	<i>37</i>

	vi
<i>Generation of Standard Curve</i>	37
<i>Reproducibility of Peptide/Matrix Spot Imaging</i>	38
RESULTS	39
<i>Discussion</i>	43
CHAPTER 4 - QUANTITATION OF THE MYELIN BASIC PROTEIN ISOFORMS ON A RAT BRAIN TISSUE SECTION.	46
INTRODUCTION	46
MATERIALS AND METHODS	47
<i>Efficiency of Trypsin Digest</i>	47
<i>Quantitation of MBP using MALDI-MRM imaging</i>	47
RESULTS	49
DISCUSSION	51
CHAPTER 5 - FUTURE WORK	55
INTRODUCTION	55
METHODS AND MATERIALS	56
<i>Overlay of light and heavy peptides</i>	56
<i>Image of Endogenous MBP peptide</i>	57
RESULTS	58
DISCUSSION	59
CHAPTER 6 - CONCLUSIONS	61
BIBLIOGRAPHY	62

List of Tables

Table 1. Reproducibility of the spot imaging method for generation of the calibration curve.....	42
Table 2. Results from the generation of three separate standard curves over a one-month period. Each ablation area represents $1963.5 \mu\text{m}^2$ of the slide.	42

List of Figures

Figure 1. Schematic Representation of a MALDI Time-of-Flight Mass Spectrometer.....	3
Figure 2 A Schematic Representation of a tandem quadrupole mass spectrometer.	8
Figure 3 Schematic representation of continuous rastering acquisition on the MALDI-QTRAP.....	9
Figure 4 Principle of MALDI imaging mass spectrometry.	13
Figure 5. Schematic of the MALDI MRM quantitation method.	19
Figure 6. <i>Protein Identification</i>	28
Figure 7 <i>Peptide Identification</i>	29
Figure 8. <i>Peptide sequence</i>	30
Figure 9. <i>Protein Sequence</i>	31
Figure 10. <i>Ion Suppression Test</i>	31
Figure 11. MALDI Images created from MRM data.....	39
Figure 12. Reproducibility of the aerosol application of peptides.....	40
Figure 13. Absolute quantitation of heavy peptide by aerosol deposition.....	41
Figure 14. <i>Efficiency of trypsin digestion</i>	49
Figure 15. <i>MALDI Images created from MRM data</i>	50
Figure 16. MALDI TOF images of the heavy and light peptides overlaid using the Labcyte Portrait 630 spotter.....	58
Figure 17. MALDI TOF image of endogenous tryptic MBP peptide and summed spectra.....	59

List Of Abbreviations

μ	micro
μl	microlitre
μm	micrometre
AAA	Amino Acid Analysis
ACN	Acetonitrile
amol	attomole
CAD	Collisionally Activated Dissociation
CHCA	α -cyano-4-hydroxycinnamic acid
DC	Direct Current
DESI	Desorption Electrospray Ionization
E_k	Kinetic Energy
Fmoc	9-fluorenylmethyloxycarbonyl
fmol	femtomole
Golli	genes of the oligodendrocyte lineage
FTICR	Fourier Transform Ion Cyclotron Resonance
H	Isotopically labelled synthetic peptide
IHC	Immunohistochemistry
IMS	Imaging Mass Spectrometry
IR	Infrared
ITO	Indium Tin Oxide
kDa	kiloDalton
L	unlabelled synthetic peptide
MCP	Micro Channel Plate
MBP	Myelin Basic Protein
MALDI	Matrix Assisted Laser Desorption Ionization
MRM	Multiple Reaction Monitoring
MS	Mass Spectrometry technique using a single mass spectrometer
MS/MS	a tandem Mass Spectrometry Technique
m/z	Mass to Charge ratio
PSD	Post Source Decay
PTMs	Post Translational Modifications
Q1	First Quadrupole
Q3	Third Quadrupole
QTRAP	Quadrupole Ion Trap
RF	Radio Frequency
SA	Sinapinic Acid
SCX	Strong Cationic Exchange
SIS	Stable Isotope-labelled Standard
SIMS	Secondary Ion Mass Spectrometry
TFA	Trifluoroacetic Acid
TLC	Thin Layer Chromatography
TOF	Time of Flight
UV	Ultraviolet

Acknowledgments

It is a pleasure to give my thanks to the people whose work has contributed to my research:

- To Dr. Christoph H. Borchers (Director of the University of Victoria-Genome BC Proteomics Centre) for the opportunity to conduct my research in a great facility with cutting-edge technology.
- To Dr. Pierre Chaurand (A leading scientist in the MALDI Imaging field) for his expertise and feedback on my research.
- To Dr. Carol Parker (Editor and writer for the University of Victoria-Genome BC Proteomics Centre) for editing this thesis and the late nights working on our journal manuscript.
- To Leanne Ohlund for being such a great teacher when I first began to learn to use the MALDI instruments.
- To Dr. Steve Evans (University of Victoria Graduate advisor) for his guidance and support.

It would not have been possible to write my thesis without the help and support of the kind people around me. My parents, Meegan and Doug Clemis, have been my biggest supporters since I began my post-secondary education. They have celebrated every 'A' with me, and consoled me when it wasn't even close. My deepest gratitude goes to Rajiv Khaneja, I would not have made it to this point without you. To you, I dedicate this thesis.

Chapter 1 - Introduction

Matrix Assisted Laser Desorption Ionization

Matrix Assisted Laser Desorption Ionization (MALDI) is an ionization technique that is used in mass spectrometry for the analysis of macromolecules. It is a two-step process of desorption and ionization of molecules that have been co-crystallized with a molar excess of matrix molecules. The matrices are usually small aromatic organic acids that have strong optical absorption in the Ultraviolet (UV) or Infrared (IR) range. The matrix solution is mixed with the analyte of interest. As the solvent is evaporated from the mixture, the analyte becomes embedded in the forming matrix crystals. Desorption is achieved through surface exposure to a brief pulse of UV or IR laser light. The matrix crystals absorb the laser energy causing the explosive desorption and ionization of the analyte into the gas phase. The matrix normally contains a strong acid, such as trifluoroacetic acid (TFA), which provides protons to the analytes during the desorption/ionization event. Essentially only singly charged ions are observed. However, some multiply charged ions can be observed when using certain matrices, like α -cyano-4-hydroxycinnamic acid (CHCA) for example, or for larger analytes like proteins (Karas et al., 2000). Both negative and positive singly charged ions are observed depending on the polarity mode of the mass spectrometer. Positive ions result from the addition of a proton or other positively charged ions, while negative ions result from the loss of a proton. The ionized molecules are accelerated in an electric field into the mass analyzer where they are separated based on the ratio between the molecules atomic mass and the number of elementary charges (m/z).

MALDI Time-of-Flight Mass Spectrometry

Principles of TOF analyzers

The MALDI source is most often coupled to a Time-of-Flight (TOF) mass spectrometer.

In a TOF instrument, the measured m/z of an ion is dependent on the time it takes for the ion to travel through a flight tube to the detector (Figure 1). The ions begin with the same amount of energy as they are accelerated by a constant electric field. The acceleration in this field results in ions of the same charge having the same kinetic energy. The velocity of an ion can be determined from the time it takes to arrive at the detector and the known distance of the flight tube. Once the ions enter the vacuum flight tube, their velocity remains fixed because it is a field-free environment. Although a heavier molecule will have a lower velocity than a lighter molecule, the kinetic energy for both is the same. The mass is solved from the known kinetic energy (E_k) and the ions measured velocity (v) using the equation $E_k = 1/2 mv^2$ (Gross, 2004).

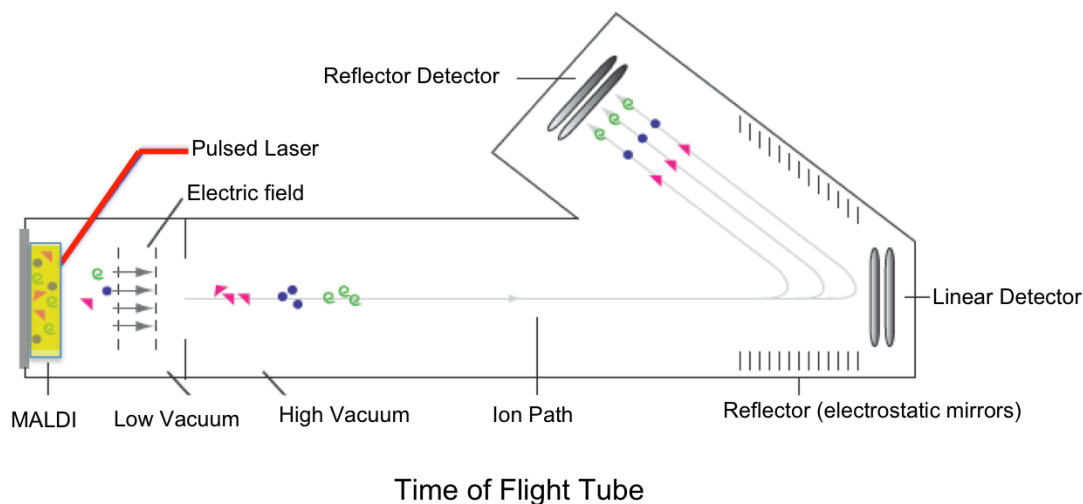


Figure 1. Schematic Representation of a MALDI Time-of-Flight Mass Spectrometer.

Under vacuum, ions (coloured shapes) travel through a field free region of the time-of-flight tube. In linear mode the ions reach the first detector in a time that is depended on their mass-to-charge ratio. Alternatively, in reflector mode, ions with the same mass-to-charge ratio but slightly different flight times travel through a set of electrostatic mirrors (the reflector), diminishing the energy spread, before hitting the second detector. Operation in the linear mode provides greater sensitivity, while operation in the reflector mode provides higher resolution. Upon reaching the detector, the ions are reported as peaks on a spectrum.

Linear, Reflector and MS/MS mode

The TOF instrument can be run in the three following mass analysis modes: linear, reflector and MS/MS. In linear mode the ions travel straight down the Time-of-Flight tube into the linear detector. The linear mode is more sensitive than the reflector mode because it is not susceptible to Post Source Decay (PSD). PSD is the fragmentation of the ions after they have entered the flight tube. In linear mode, all the fragmentations resulting from PSD reach the detector at the at the same time as the intact ion, regardless of their size or whether or not they retained the charge (Gross, 2004). In reflector mode the ions travel down the same ion path as in linear mode towards the reflector. At the

reflector, the ions penetrate into the electrostatic mirrors until they reach zero kinetic energy, they are then expelled out towards a second detector. This affectively increases the Time-of-Flight tube relative to the linear mode. The increased distance the ions travel results in increased signal resolution because there is more time for the separation of ions that have different m/z ratios. However, the major source of the increased signal resolution by the reflector mode is from the penetration of the ions into the electrostatic mirror. Ions with the same m/z ratio can have variations in their flight times due to differing kinetic energies resulting from events during desorption/ionization that lead to different initial velocities. The mirror is essentially a decelerating electric field that compensates for the initial energy spread. Ions with more energy than their isobaric counterparts will fly deeper into the mirror, spending more time in the reflector so that they all reach the second detector closer together in time. The reflector mode has better resolution, but less sensitivity than the linear mode. PSD fragments without a charge will not be reflected. Additionally, the charged PSD fragments have a smaller mass than their precursor, so they do not penetrate the mirror as deeply, so they have a shorter flight path and arrive earlier to the reflector detector.

When two of these analyzers are put in tandem, it is possible to acquire more information about a particular ion using the MS/MS mode. In MS/MS mode the first flight tube isolates a particular ion using a based on the arrival time at the end of the first time of flight tube. Next, the selected ions are broken up (fragmented) in a collision cell before being passed to the second TOF analyzer where the fragments are separated according to their m/z ratio. The resulting MS/MS spectrum consists of signals that are only from

product ions of the selected precursor. The selection of ions in the first TOF analyzer and the analysis of the fragments in the second is the basis for molecular identification.

Peptide sequencing is a common use for TOF/TOF mass spectrometry. A precursor peptide is selected for sequencing based on its m/z ratio. In the collision cell, peptides break apart at characteristic bonds along the peptide-backbone (Roepstorff et al., 1984). Each breakage results in one neutral fragment and one charged fragment, only the charged fragment will be analyzed by the second mass spectrometer. The m/z ratios of the fragment ions are recorded, and can be used to determine the amino acid sequence of the precursor peptide. The most common breakage point is at the CO-NH peptide bond. Named using Roepstorff nomenclature (Roepstorff et al., 1984), the resultant N-terminal fragments, that retained the charge, are called b ions, and the C-terminal fragment ions are called y ions. The mass difference between two adjacent b ions, or two adjacent y ions, corresponds to a particular amino acid. Tandem mass spectrometers do not always use the second mass spectrometer. Both the linear and reflector modes can be used on a tandem TOF/TOF instrument using only one of the mass spectrometers. The abbreviation 'MS' is used when only one mass spectrometer is used in the analysis.

Detector

Ions reach the detector after passing through the mass analyzer. The most common type of detector is based on signal amplification by an electron multiplier. A micro channel plate (MCP) is a porous solid core with millions of tiny channels that have a semi-conductive coating inside. When an ion strikes one of these channels with an electric potential, it causes secondary electrons to be released. These secondary electrons then

trigger more electrons to be released as the electric field forces them to hit the wall of the channel and release even more secondary electrons in a chain reaction resulting in signal amplification; this is known as the cascade effect. The gain of a single MCP is 10^3 - 10^4 , however, often two MCPs are put together to increase the gain to 10^6 - 10^7 (Gross, 2004).

Bruker Ultraflex III ion source

The Bruker Ultraflex III is a tandem TOF mass spectrometer that is one of the primary instruments used in the experiments described in this thesis. It is equipped with a neodymium-doped yttrium aluminium garnet (Nd:YAG, $\text{Nd:Y}_3\text{Al}_5\text{O}_{12}$) solid state laser with a repetition rate of 200 Hz. The focus size of the laser is computer controlled and ranges between 10-80 μm . The laser system provides pulsed UV light on to a small spot on the target. An automated method allows for the continuous collection of data from a sample by rastering the laser over the target in a stop-and-start manner, where the laser is halted during each data acquisition. This is the basis for MALDI-TOF imaging, and will be explained in detail below.

Triple Quadrupole Mass Spectrometer

Principles of MALDI triple quadrupole analyzers

The MALDI triple quadrupole mass spectrometer is another type of tandem mass spectrometer. Ion separation is based on the stability of their trajectories in oscillating electric fields. It consists of three linear sets of four circular rods set in parallel to each other. Each opposing pair of rods is connected electronically and emits either a direct current (DC) or radio frequency (RF). In each of the three sets of quadrupoles, the ions

travel between the four rods as the rods scan through different frequencies, only ions with a certain m/z value will pass through for a given ratio of voltages; all others will collide with the rods.

MS/MS and MRM

In MS/MS mode, the first (Q1) and third (Q3) set of quadrupoles act as separate mass spectrometers; the middle, which uses only RF frequency, acts as a field free region. Q1 and Q3 act as mass filters, and the middle is often used as a collisionally activated dissociation cell (CAD) (Figure 2). Multiple reaction monitoring (MRM) is an MS/MS scan mode that is capable of sensitive, quick, and specific quantitation of analytes from a complex sample (Kondrat et al., 1978). MRM is a targeted approach that requires knowledge of the molecular weight of both the precursor ion and its product fragment. Precursor ions with a specific m/z ratio are isolated in Q1, these ions pass to the CAD where they collide with a gas causing them to fragment at characteristic bonds (as described above). The fragments then pass to Q3, where a specific product fragment is selected for passage to the detector. The pair of selected m/z ratios of the precursor and product ions is called a transition, and is the basis for MRM. During a MRM experiment the ion currents associated with the selected transitions are monitored. The intensity of the ion current reaching the detector is a quantitative indicator of the target analyte that is represented by the transition. MRM experiments give high levels of both sensitivity and specificity in the quantitation of analytes from a complex sample.

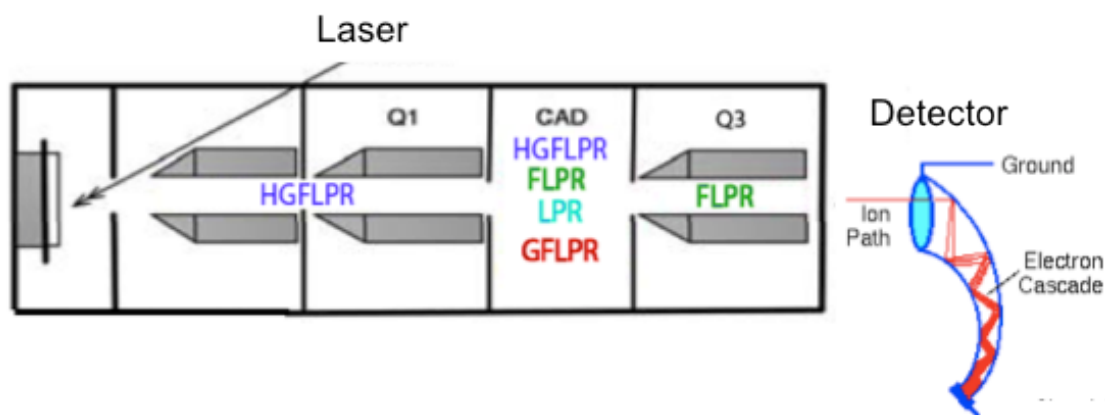


Figure 2 A Schematic Representation of a tandem quadrupole mass spectrometer.

A triple quadrupole consists of a linear series of three sets of four circular rods. The first (Q1) and the third (Q3) quadrupoles act as mass filters. The middle quadrupole (CAD) is a collision cell for ion fragmentation. The ions pass through the sets of quadrupoles to the channel electron multiplier (CEM) detector.

The Applied Biosystems MALDI QTRAP 4000

The Applied Biosystems 4000 QTrap mass spectrometer is equipped with a vacuum MALDI source with a nitrogen laser that has a repetition rate of 1000 Hz. The QTRAP 4000 can operate either as a triple quadrupole or as an ion trap. An automatic method can be employed to collect large amounts of data. This is described schematically in figure 3, and is the basis for MALDI-QTRAP MRM imaging experiments described below. A sample is moved continuously in a serpentine pattern relative to the laser. The high-frequency laser results in effectively continuous ablation and data accumulation. As the ions are ablated, each ion transition chosen for analysis is selected for detection with a 50-ms dwell time. With a scan speed of 0.9 $\mu\text{m}/\text{ms}$, the laser moves across 45 μm of sample during the 50-ms dwell time. A 1000 Hz laser results in 50 shots summed per transition. Including a 5 ms settling time, the laser moves across 247.5 μm of sample

while signals from up to five transitions is being acquired, with each ion being sequentially detected within a lateral distance of 45 μm .

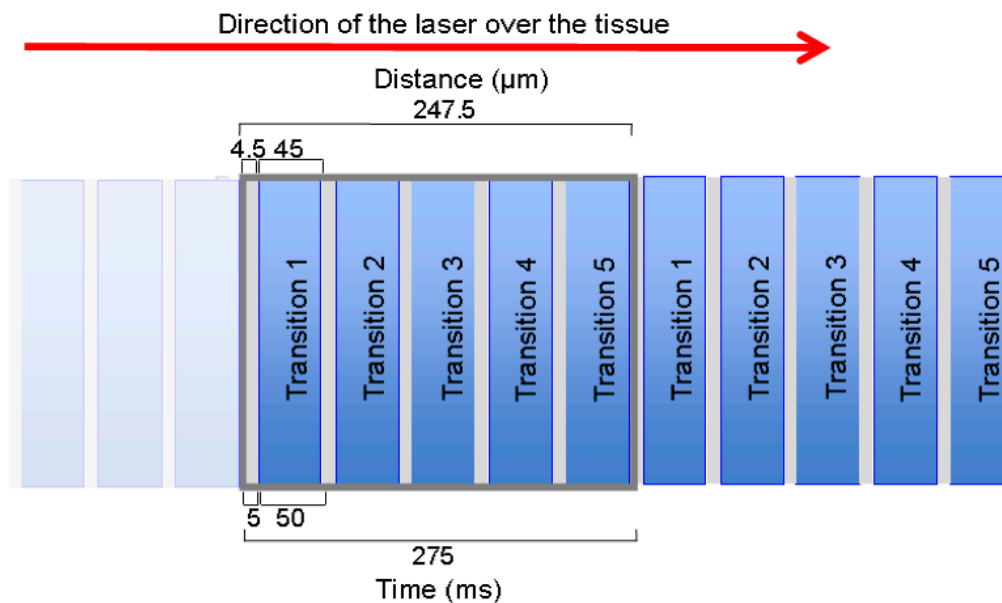


Figure 3 Schematic representation of continuous rastering acquisition on the MALDI-QTRAP.

The 1000-Hz laser is pulsed without pause while the plate is moved continuously. The continuous ablation results in an effectively constant stream of ions into the mass spectrometer. Each transition is detected as the laser is travelling a discrete distance across the sample (45 μm). With a scan speed of 0.9 $\mu\text{m}/\text{ms}$ and a dwell time of 50 ms, 50 laser shots are summed as the laser (diameter = 200 μm) travels over 45 μm of sample. There is a 5 ms settling time between transitions during which the laser moves an additional 4.5 μm . The laser travels across 180 μm of sample to collect the data for each set of 4 transitions during which time analyte signals are detected, and then an additional 45 μm for the detection of the alignment line transition. This results in a 275-ms duty cycle, which then repeats.

Detector

The detector on the QTRAP 4000 is a channel electron multiplier (CEM). Like the MCP detectors, it uses the cascade effect for signal amplification. Unlike the MCP, it is a single continuous curved tube. These detectors provide gains of up to 10^8 (Gross, 2004).

Mass Spectrometry-Based Tissue Imaging Methods

Imaging mass spectrometry (IMS) is a technique used to visualize the spatial distribution of a variety of different compounds in thin tissue sections based on the molecular masses.

There are essentially four steps in the process of IMS: sample preparation, desorption and ionization, mass analysis, and image registration.

The sample preparation procedure depends on the method of desorption and ionization.

In IMS the three most common methods of desorption and ionization of biomolecules are secondary ion mass spectrometry (SIMS), desorption electrospray ionization (DESI), and matrix assisted laser desorption/ionization (MALDI). Desorption and ionization by

SIMS-IMS utilizes a primary ion beam of metal or C_{60} ions to produce secondary ions from the surface of a sample, which are then directed into the mass analyzer. Desorption and ionization by DESI uses energetic, charged electrosprayed solvent droplets that are directed toward the sample surface. The charged droplets hit the sample and dissolve the analytes. Ions are formed upon desolvation in a manner analogous to electrospray

ionization. In MALDI-IMS desorption and ionization occurs as described above following several steps of sample preparation. If proteins or peptides are the analytes of interest, the tissue samples are washed with a series of alcohol rinses to remove compounds that can interfere with analysis and to locally fix the analytes to the slide.

The tissue is then homogeneously coated with a matrix that is suitable for MALDI.

Following the desorption and ionization by the three methods described above, the ions are separated based on their mass to charge ratio (m/z) inside the mass analyzer. The mass analyzers can be a linear quadrupole ion trap, a quadrupole time of flight, a Fourier transform ion cyclotron resonance (FTICR), an Orbitrap™, or a TOF instrument that has been interfaced with a source for desorption/ionization. Each type of instrument has different mass spectrometric qualities and characteristic performance indicators, such as mass resolving power and m/z range. In an IMS experiment, the whole surface of the sample is analyzed and a spectrum is acquired at each of a regular series of positions across a section of tissue. Each spectrum contains molecular weight and abundance information that is representative of the analytes present at that position. Specific ion density images can then be generated from a plot of the abundance of any ion measured, as a function of individual pixel location.

MALDI Imaging

MALDI-IMS was first introduced as a method for imaging biological samples in 1997 (Caprioli et al., 1997). Since its introduction, there have been rapid developments in the methodologies, instrumentation and the software used in this technique. MALDI imaging has many useful applications, for example, in cancer research it can be used to identify tumor type, grade, stage, and surgical margins (Chaurand et al., 2004).

Visualization of aberrant molecular pathology between healthy and diseased tissue can be used for biomarker discovery (Meistermann et al., 2006). In addition, it is possible to apply this technology to the imaging of drugs and their metabolites simultaneously, in order to determine the site of action and to track the distribution of the analytes over a

period of time (Reyzer et al., 2003; Troendle et al., 1999). The matrix is deposited on to the tissue in either a thin layer or in a spot pattern. As the solvent is evaporated from the matrix solution, the analytes in the tissue are extracted into the forming matrix crystals.

During MALDI-IMS the laser is rastered across the surface of the matrix coated tissue, desorbing and ionizing the biomolecules in its path (Figure 4). Hundreds of intact peptides and proteins can be detected directly from tissue using this method. The MALDI method is sensitive and is tolerant of salts and other contaminants. The high sensitivity of the MALDI-IMS method was demonstrated in an experiment using a brain section spotted with a dilute solution of insulin. The insulin spot had a concentration of 12 fmol/mm², therefore, the laser with a diameter of 50 µm resulted in the detection of 25 amol per ablation area, showing the capability for the detection of biomolecules present in tissue sections (Chughtai et al., 2010; Sanchez et al., 2004).

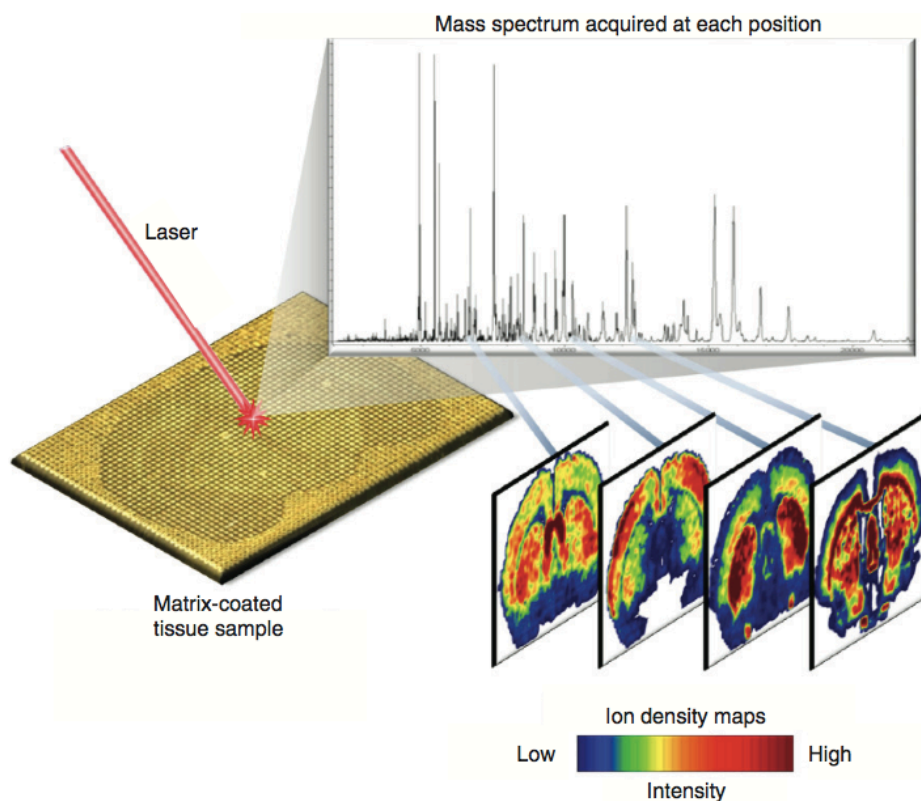


Figure 4 Principle of MALDI imaging mass spectrometry.

A thin tissue section is moved in two dimensions while an individual mass spectrum is recorded systematically for every x-y coordinate (image adapted from Castellino et al., 2011).

Advantages and limitations of MALDI imaging

In addition to the major advantage of maintaining the spatial information, another advantage of MALDI-IMS over traditional mass spectrometry based analytical methods using tissue homogenization, is the avoidance of time consuming extraction, purification, or separation steps which can often produce experimental artifacts. Information acquired from the basic images generated using IMS is similar to those from immunohistochemistry (IHC). However, unlike IHC, there is no need for antibodies or prior knowledge of the protein profile. The IMS method is not limited to proteins, many other biological analytes, such as lipids, peptides, and metabolites, can all be detected.

A mass spectrometry based approach for the analysis of biological samples has some limitations. It is very important that sample preparation is done quickly and carefully to decrease analyte delocalization and degradation, which can affect the data reproducibility. MALDI imaging provides a qualitative picture of analyte distribution. However, even when the application of the matrix onto the tissue is homogenous, the formation of the matrix crystals is not. These crystals can differ in density per unit surface, size, quality, and analyte extraction efficiency, depending on the local physical properties within the tissue section. The inconsistencies in matrix crystal formation can result in errors in determining the abundances of the analytes, leading to incorrect conclusions about their distributions.

The standard approach for mitigating these matrix effects is normalization based on the total ion current (TIC) (Alfassi, 2004; Rasmussen et al., 1979). Total Ion Current Normalization is performed by summing all of the intensities in each spectrum and obtaining a total intensity value for each spectrum. These totals are then averaged. Each intensity value within a spectrum is then multiplied by the ratio of its total intensity to the average total intensity. This normalizes the spectrum because, after this process, the total ion intensity for each spectrum now equals the average total intensity. This normalization method, however, has several limitations with respect to relative quantitation. For example, the whole analysis can be rendered less sensitive because large signal intensities are the greatest contributors to the TIC normalization of spectra. Often these large signals fluctuate dramatically from sample to sample and can, at times,

even be saturated. Furthermore, if intense signals from ions that are not clinically relevant are more common in one clinical group than another, then TIC normalization will lead to over-training during classification and will inappropriately suppress all signal intensities in the group (Duncan et al., 2008).

In solution-based analyses, normalization against a reference peak can correct for matrix effects on the analyte signal. In MALDI imaging, there is the additional challenge that it is also necessary for the standard to be homogeneously distributed on the surface of the tissue section. If a uniform and homogenous distribution can be achieved, successful normalization can be performed.

In addition to the above-mentioned matrix effects, the ion signals from competing endogenous species, such as lipids and other blood compounds, may cause significant suppression of the signal from the analyte of interest; this is known as ion suppression. When one analyte is present in greater amounts or ionizes more easily than others, ion suppression will occur. Biological tissue is very complex, composed of many analytes with different properties and proton affinities. Ion suppression can be minimized during the sample preparation stage. For example, tissue sections used for protein analysis are washed in a series of alcohol solutions to remove salts, lipids and other contaminants that could lead to protein signal suppression (Seeley et al., 2008).

Bruker ImagePrep Station

The Bruker ImagePrep station is a push button device for the aerosol deposition of liquids onto thin sections of tissue. The Imageprep is a spray chamber that is completely decoupled from the outside humidity. The chamber is flushed with nitrogen, removing oxygen from the system to prevent sample oxidation and to obtain reproducible experimental conditions. A liquid is gravity fed onto a porous metal film that is vibrated by current flow through an attached piezoelectric sheet. A dense nebulized mist created by this vibrational vaporization settles onto the tissue section. The average diameter of the droplets that make up the mist is 20 μm . Because of the small droplet size, the location of the analytes is maintained within the tissue. The ImagePrep station can be run automatically using a preinstalled method, or in manual operation mode where the parameters are set prior to each experiment. The settings in manual mode determine the number of spray cycles, as well as the power and modulation of the spray. The user also defines the duration of the spray, the incubation time and the drying time during each of the cycles. During the incubation period there is no spray or active drying. The spray chamber is almost saturated with solvent vapour while the droplets incubate on top of the tissue. Following the incubation, the samples are dried with a constant flow of nitrogen gas. In the experiments described in this thesis, I use the ImagePrep Station for the enzymatic digestion of coronal sections of rat brain, the deposition of an isotopically labelled standard and for the application of the MALDI matrix.

Quantitative MALDI imaging

To better understand the biological functions of different regions within a tissue, it is advantageous to determine the location and abundance of the constituent proteins. Mass spectrometry has proven invaluable for the absolute quantitation of proteins in solutions such as plasma and tissue homogenates; however, important anatomical information is lost when tissue samples are homogenized before protein quantitation. It would therefore be beneficial to have a quantitation method that would maintain this spatial information.

In-situ trypsin digestion allows the resulting peptide fragments to remain close to their point of origin in the two-dimensional space of a tissue slice. Trypsin is a proteolytic enzyme that cleaves a peptide chain at the carboxyl side of lysine and arginine, with the exception of when either residue is followed by proline. In MRM mode, the resulting tryptic peptides along with the uniformly-deposited stable isotope-labelled peptide analogs can be monitored for the accurate quantitation of the protein of interest. MRM-based MALDI imaging has increased specificity through the precise selection of a targeted mass in the first quadrupole, and a specific fragment ion mass in the third quadrupole. A peptide based method is employed for the quantitation of proteins because the triple quadrupole mass spectrometer, that is capable of MRM analysis, has an upper m/z limit of 4000 (Gross, 2004). Ionization by MALDI usually results in a singly charged ion, therefore, most proteins would be outside of this m/z range. Furthermore, it would be impractical to make a labelled protein for use as an internal standard.

Previously, MRM based MALDI imaging has been used to map the localization of the drug Moxifloxacin and a reference standard in infected rabbit lung biopsies to determine the penetration of the drug into granulomas (Prideaux et al., 2011). The reference standard used in this study was another fluoroquinolone compound that was applied by hand with a Thin Layer Chromatography (TLC) sprayer. This study did not attempt to quantitate the analyte of interest directly from the tissue, however, they were able to improve sensitivity and selectivity with the MRM method that enabled detailed drug localization within the granuloma that could not be determined by alternative methods (Prideaux et al., 2011).

I Present a new MALDI-MRM based IMS approach for the absolute quantitation of proteins present in thin tissue sections after *in-situ* enzymatic digestion. The quantitative imaging method used in my study involves an *in-situ* trypsin digestion, followed by uniformly spraying the tissue sample (using an automated spray device) with an isotopically-coded peptide that is representative of the protein of interest, matrix application, and MALDI MS analysis (Figure 5). The labelled peptide acts as an internal standard for the endogenous tryptic peptide. The majority of the content presented in this thesis is based on the published article in Analytical Chemistry by Clemis et al. (2012). My hypothesis is that a method based on MRM with isotopically-labelled internal standards can be developed, that will allow the accurate quantitation of proteins in MALDI Imaging.

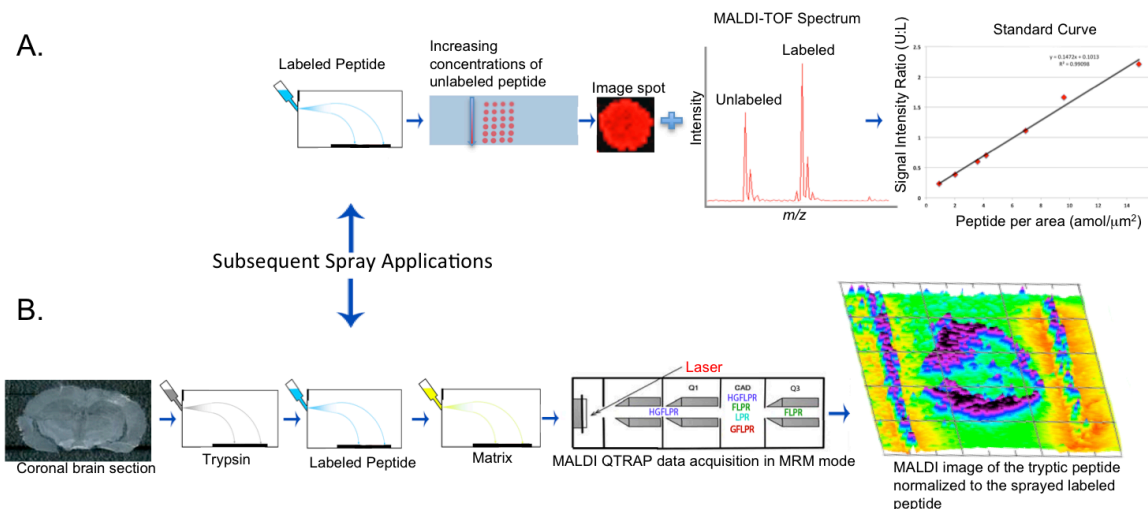


Figure 5. Schematic of the MALDI MRM quantitation method.

A. Absolute quantitation of heavy-arginine labelled peptide by aerosol deposition. The labelled peptide is deposited onto the conductive ITO coated glass slide. A $0.5\text{-}\mu\text{L}$ aliquot of the synthetic unlabelled version of the sprayed peptide in matrix is spotted onto the slide in increasing concentrations. Ion images of the spots are obtained in reflector positive mode of a MALDI-TOF mass spectrometer. The area of each spot is calculated to determine the amount of unlabelled peptide per ablation area. This is then plotted against the average ion signal intensity ratio of the unlabelled to labelled peptide over the area of the spot in order to generate a standard curve.

B. Peptide Image of endogenous myelin basic protein. A thin slice of flash frozen tissue is thaw mounted onto a conductive ITO coated glass slide. Trypsin, labelled peptide, and matrix are applied separately, using aerosol deposition. Ion images are created from the MRM data obtained on a MALDI-QTRAP mass spectrometer. The ion displayed is from the endogenous tryptic peptide.

Chapter 2 - Protein characterization and synthesis of a representative peptide.

Introduction

There are many protein identification methods that use mass spectrometry. The most common and well-established approach is the bottom-up strategy (Cui et al., 2011). This method is used to identify proteins based on the amino acid sequences of peptides generated by enzymatic cleavage. Prior to digestion, proteins in a complex mixture can be separated by gel electrophoresis, capillary electrophoresis, SCX (strong cationic exchange), or by liquid chromatography to minimize the complexity. However, separation can also be done at the peptide level, using the same methods, but after the digestion step. In this case, the chromatographic separation can be performed on-line when coupled to an electrospray mass spectrometer.

Characteristic peptide fragments are created when a protein is digested with a proteolytic enzyme like trypsin. If the amino acid sequences in these tryptic peptides are unique to a protein of interest, the quantity of an individual fragment will reflect the quantity of the protein. The amino acid sequences of the peptides can then be determined with the use of a tandem mass spectrometer. The peptide mass spectra are compared to theoretical peptide masses calculated from a proteomic database, using a search engine such as Mascot (Perkins et al., 1997) to identify the original proteins in the sample.

The theory behind the bottom-up strategy has been applied to MALDI imaging for protein identification from tissue sections. In a recent publication, 14 peptides originating from four proteins were identified directly from on-tissue MS/MS experiments on a trypsin digested rat brain section (Schober et al., 2011).

The proof-of-concept experiments outlined in my study demonstrate the feasibility of a MALDI imaging platform that begins with protein identification and ends with the quantitation of the discovered protein. This design assumes that the enzymatic digestion is complete. Quantitation of a protein based on a representative peptide is a common application in mass spectrometry (Ong et al., 2005). Once a suitable peptide representative of the protein of interest is identified, it is necessary to acquire a labelled version of this peptide in a known amount to use as an internal standard. For absolute quantitation, the labelled version must have the same ionization properties and behave identically to the endogenous tryptic peptide in the mass spectrometer. An internal standard is important because the absolute intensity of an ion signal in a mass spectrum is a poor indicator of the amount of analyte present, but ratios of ion signal intensities between an analyte and an isotopically-labelled standard of the same analyte accurately reflect differences in their abundances (Jiang et al., 2007).

Although the bottom-up strategy assumes complete and reproducible digestion, there are problems when quantitation is based on intact proteins. Proteins can be present in many possible forms due to post-translational modifications (PTMs). This can make quantitative assays which depend on antibody interaction problematic due to blocking of

the epitope and potential cross-reactivity issues with non-target proteins. Moreover, some proteins can have many PTMs, and these may be time and location dependent. This can cause large variations in the mass of the proteins, which makes the analysis of full proteins by mass spectrometry difficult.

The lower m/z range of the more sensitive mass spectrometers typically used in quantitative proteomics further impedes the analysis of intact proteins. For example, the Applied Biosystems QTRAP 4000 is reported by the company to have an m/z range of 5 – 4000, which makes it useful for small molecule, drug, metabolite, and peptide analysis.

In my study, we performed a quantitative analysis of myelin basic protein isoforms (MBPs) in rat brain, using bottom-up proteomics and MALDI imaging. MBPs are the major protein component of myelin, the electrically insulating material that forms a layer around the axon of a neuron. There are several MBP isoforms that all arise from differential transcription initiation and splicing from the Golli (genes of the oligodendrocyte lineage) gene complex during different stages of neural development (Campagnoni et al., 2004). The MBP isoforms, which range from 14 to 21 kDa, are encoded from the major alternatively-spliced MBP mRNAs (Kamholz, 1988; Roth, 1987). The most abundant of MBPs in mature rats are the 14-kDa and 18.5-kDa isoforms, these two species comprise more than 70% of the total MBPs in the rat proteome (Akiyama et al., 2002).

Materials and Methods

Protein Image

A rat brain tissue sample that had been snap frozen (Pel-Freez, Rogers, Arkansas) was sectioned into 12 μm slices on the Thermo Fisher Scientific Microm HM500 cryostat (Waltham, MA.) and thaw mounted onto conductive ITO coated glass slides. The slide was placed in a vacuum for 60 min to allow the tissue section to dry and equilibrate to room temperature. The slide was rinsed in a series of alcohol and water solutions -- 1 x 15 seconds in 70% ethanol and 1 x 15 seconds in 90% ethanol: 9% acetic acid (v/v). The tissue was coated with 20 mg/mL sinapinic acid (SA): 70% ACN: 0.1% TFA (v/v) using the Bruker ImagePrep station with the following settings in manual mode: cycles = 45, power = 20, modulation = 10, spray = 1s, incubation = 60s, and dry = 100s. The data was acquired using Bruker's flexControl and flexImaging software using the Bruker Ultraflex. flexControl is the user interface for instrumental control of the mass spectrometer and is used to acquire spectra. Working in conjunction with flexControl, flexImaging is used to acquire and analyze the spectra collected from imaging experiments. It is composed of a graphical run editor and an analysis/visualization component. The MALDI-TOF MS was run in linear mode with a pixel resolution of 150 μm and 200 shots per pixel.

Peptide Image

The sample preparation was the same as for the protein image until after the wash steps. Following the wash, the tissue was digested with trypsin. The trypsin was purchased

from Promega (Madison, WA) and was rehydrated with 100 mM ammonium bicarbonate to a final trypsin concentration of 46 $\mu\text{g}/\text{mL}$. The trypsin was applied to the tissue using the Bruker ImagePrep workstation in manual mode using the following optimized settings: cycles = 30, power = 20, modulation = 10, spray = 1s, incubation = 60s, and dry = 100s. This method repeatedly sprays small amounts of the trypsin solution onto the tissue and incubates for 80 minutes at room temperature ($\sim 22^\circ\text{C}$) in a humid environment. The sprayed trypsin appeared to dry completely between each successive application. Following the application of trypsin, 10 mg/mL CHCA in 70% ACN/ 0.1% TFA, was applied using the same manual settings as the SA matrix for the protein image. The CHCA was purchased from Sigma-Aldrich (St. Louis, MO) and re-crystallized. The data was acquired on the Bruker ultraflex III and was analyzed using the following software applications: Bruker flexControl and flexImaging. The MALDI-TOF MS was run in reflector mode with a pixel resolution of 125 μm and 200 shots per pixel.

Peptide Identification

The three ion signals that had a similar spatial morphology to the 14 kDa and 18.5 kDa signals were chosen for MS/MS mode analysis on the Bruker ultraflex III in MS/MS mode using the flexControl application. The Biotoools software application, also from Bruker, was used to interface with Mascot for amino acid sequence identification for the chosen ion signals. Mascot is a software package that compares submitted spectra data from an MS/MS experiment to a database of known proteins and reports the most probable protein identity (Perkins et al., 1997). The sequences were then put into

BLASTp, an algorithm used to compare an amino acid query sequence against a protein sequence database (Altschul et al., 1990).

Synthesis of Light (L) and Heavy (H) Peptides

A tryptic peptide from rat myelin basic protein (HGFLPR) was synthesized with and without a stable-isotopically coded $^{13}\text{C}_6$ $^{15}\text{N}_2$ L-arginine residue (+10 Da) at the University of Victoria-Genome BC Proteomics Centre, Victoria, Canada (Kuzyk et al., 2011; Kuzyk et al., 2009). The peptides were synthesized on a Prelude peptide synthesizer (Protein Technologies, Tucson, AZ) at a scale of 5 μmol using 9-fluorenylmethyloxycarbonyl (Fmoc) chemistry. The C-terminal amino acids for the unlabelled peptides were conjugated to a Wang resin (Sigma-Aldrich, St. Louis, MO) and the C-terminal amino acids for the labelled peptide were conjugated to TentaGel R resin (Rapp Polymere). Subsequent residues with a concentration of 100 mM, were double coupled using 20% piperidine as the deprotector, and 1H-Benzotriazolium 1-[bis(dimethylamino)methylene]-5chloro-hexafluorophosphate (1),3-oxide (HCTU) as the activator. The fully-synthesized peptides were cleaved online using 95:2.5:2.5 trifluoroacetic acid (TFA): water: triisopropylsilane (Sigma-Aldrich, St. Louis, MO) and subsequently removed from the synthesizer. Under a stream of nitrogen, the volume of TFA in the samples was reduced. Pellets were formed by precipitation with ice-cold diethyl ether (Sigma-Aldrich, St. Louis, MO) and centrifugation at 13000 rpm for five minutes, and then pipetted for removal of the ether layer. The pellets were resolubilized in 0.1% TFA and lyophilized (Modulyod, Thermo Savant).

The labelled and unlabelled peptides were purified using the Ultimate 3000 (Dionex, Sunnyvale, CA), a High Performance Liquid Chromatography (HPLC). Elution of the peptides was monitored at 230 nm. Approximately 5 mg of the crude peptides were chromatographed using a monolithic C₁₈ (218TP) reversed-phase column (10 x 250mm, 10µm resin) with a linear gradient of 0.1% TFA in water (v/v) and 0.85% TFA at a flow rate of 4 mL/minute over 25 minutes. The fractions thought to contain the peptides were spotted onto a MALDI plate and covered in 3 mg/mL CHCA in 60% ACN / 0.1% TFA. The spots were analyzed using the Bruker ultraflex III. The fractions that had a purity of 80% or higher, determined by the MALDI-TOF analysis, were pooled and lyophilized. Prior to lyophilization, a small portion of the sample was taken for Amino Acid Analysis (AAA) at the Facility for Sick Children in Toronto, Ontario. AAA is used to determine the concentration of the synthesized peptides.

Test for Ion Suppression

A 1-µL aliquot of a 1:1 ratio of 0.5 pmol/µL of the light and heavy MBP peptides was spotted onto an ITO coated glass slide. A 1-µL aliquot of matrix solution (10 mg/mL CHCA in 70% ACN/ 0.1% TFA) was then spotted on top of the dried peptides. Two 10 µm sections of liver tissue were fixed onto two ITO coated glass slides and were placed in a vacuum for 60 min to allow the tissue sections to dry and equilibrate to room temperature. The sections were rinsed in a series of alcohol and water solutions -- 1 x 15 seconds in 70% ethanol and 1 x 15 seconds in 90% ethanol: 9% acetic acid (v/v). One slide was digested with trypsin using the same protocol described above. Following the digestion, the labelled and unlabelled peptides were spotted onto the tissue and covered in

matrix using the same method as described above for the glass slide. This was also done for the liver tissue on the third slide that was not digested with trypsin.

Results

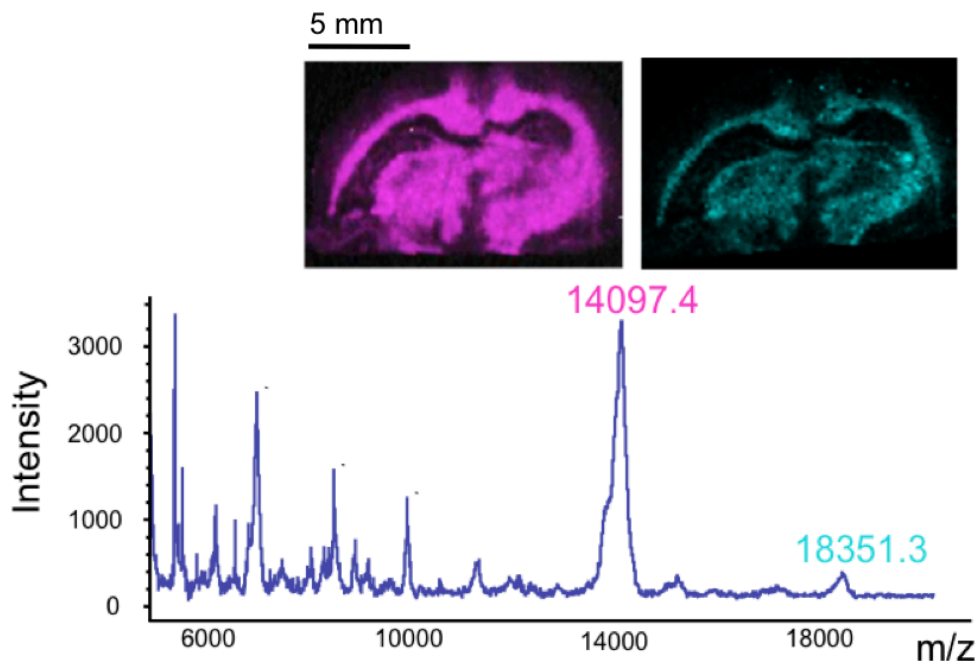


Figure 6. *Protein Identification*

Distribution of ions detected at m/z 14097.4 and 18351.3 from a coronal rat brain section and a summed ion spectrum analyzed in linear positive mode TOF, using SA as the matrix. The IMS data was acquired with a spatial resolution of 150 μm .

The summed ion spectrum (Figure 6, bottom) from a full tissue analysis of a coronal section of rat brain shows two ion signals, m/z 14097.4 and m/z 18351.3, that have almost identical distribution profiles (Figure 6, top). The ion signals for the 21.5 kDa and 17.0 kDa MBP isoforms were not observed in this analysis.

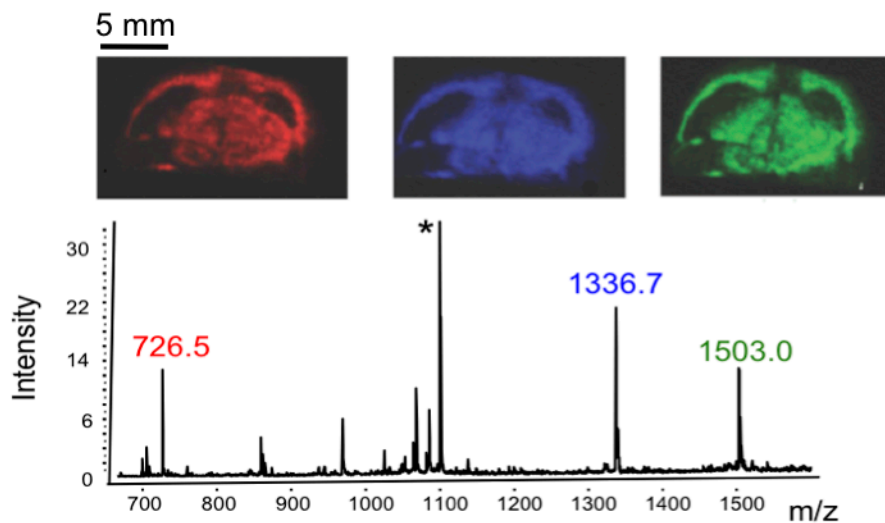


Figure 7 Peptide Identification.

Ion images corresponding to signals with m/z 726.5, m/z 1336.7 and m/z 1503.0 from a coronal rat brain tissue section after digestion with trypsin, and coating with CHCA. The IMS data was acquired in reflectron TOF with a spatial resolution of 125 μm .

The three ion images from the digested coronal section of rat brain (Figure 7 top) display a similar distribution to the m/z 14097.4 and 18351.3 ion images. All three ion signals result in almost identical expression profiles. The base-peak (*) at m/z 1090.6 has been previously identified as a tryptic peptide from PEP-19 (AAVAIQSQFR), by Groseclose et. al. (2007).

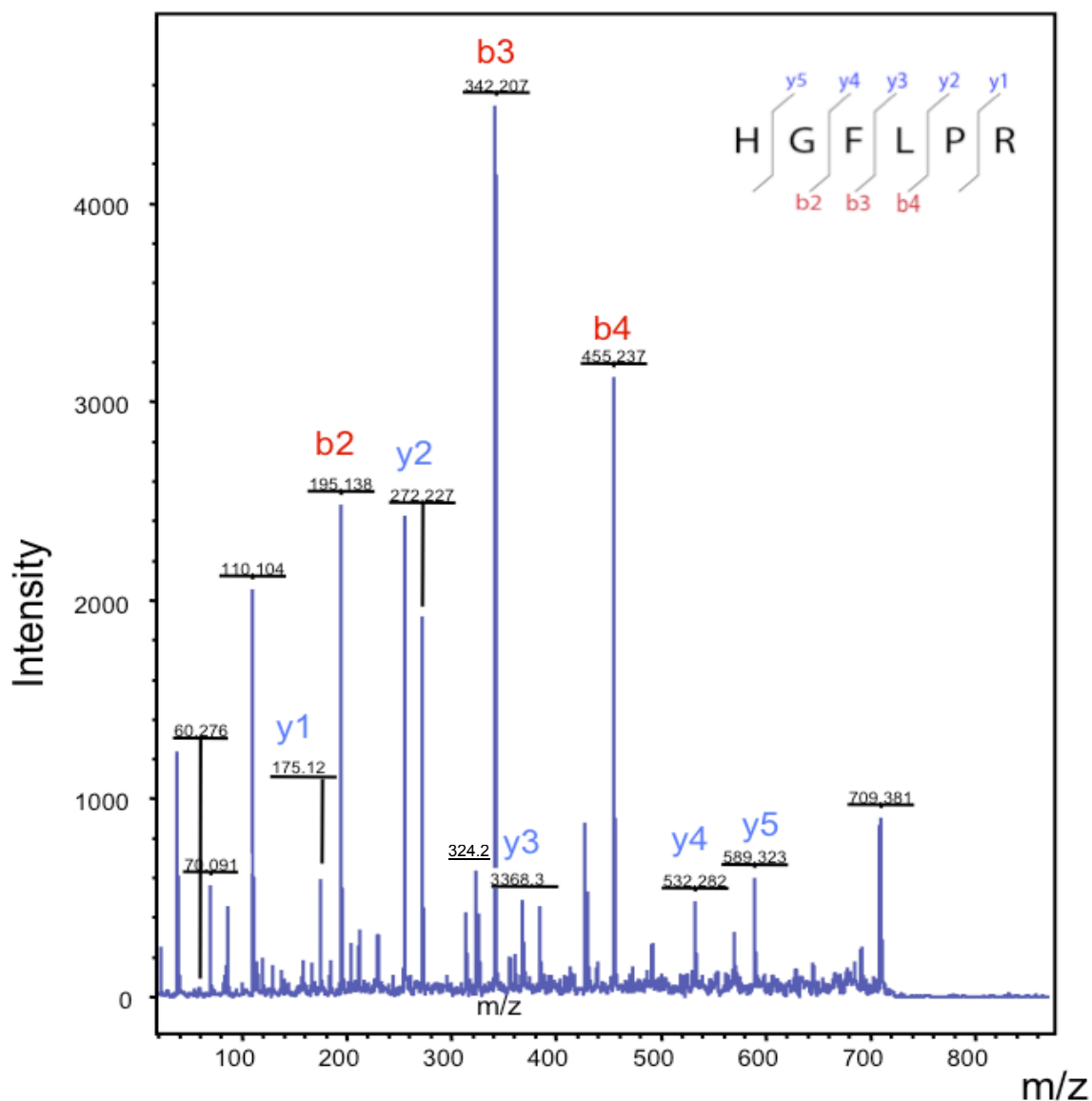


Figure 8. Peptide sequence.

One of the three MS/MS spectra acquired directly from the tissue following trypsin digestion and CHCA matrix coverage.

MS/MS analysis (Figure 8) followed by database searching and sequence identification using the Mascot database search engine (and the Swissprot *Rattus norvegicus* database), identified the three endogenous tryptic peptides to be: HGFLPR (m/z 726.5), YLATASTMDHAR (m/z 1336.7), and TTHYGSLPQKSQR (m/z 1503.0).

>gi|4454315|emb|CAA10806.1|myelin basic protein [Rattus norvegicus]
 MASQKRPSQRHGSKYLATASTMDHARHGFLPRHRDTGILDSIGRFFSGD
 RGAPKRGSGKDSHTRTTHYGSLPQKSQRTQDENPVVHFFKNIVTPRTPP
 PSQGKGRGLSLSRFSWGAEGQKPGFGYGGRASDYKSAHKGFKGAYDA
 QGTLSKIFKLGGRDSRSGSPIARR

Figure 9. Protein Sequence.

The MS/MS sequence data from all three ions was searched against the *Rattus norvegicus* database using BLASTp.

The m/z 14097.4 and 18351.3 ion signals were identified as myelin basic protein isoforms 4 and 2, respectively. The results of the BLASTp search also showed that these sequences were unique to the MBP isoforms.

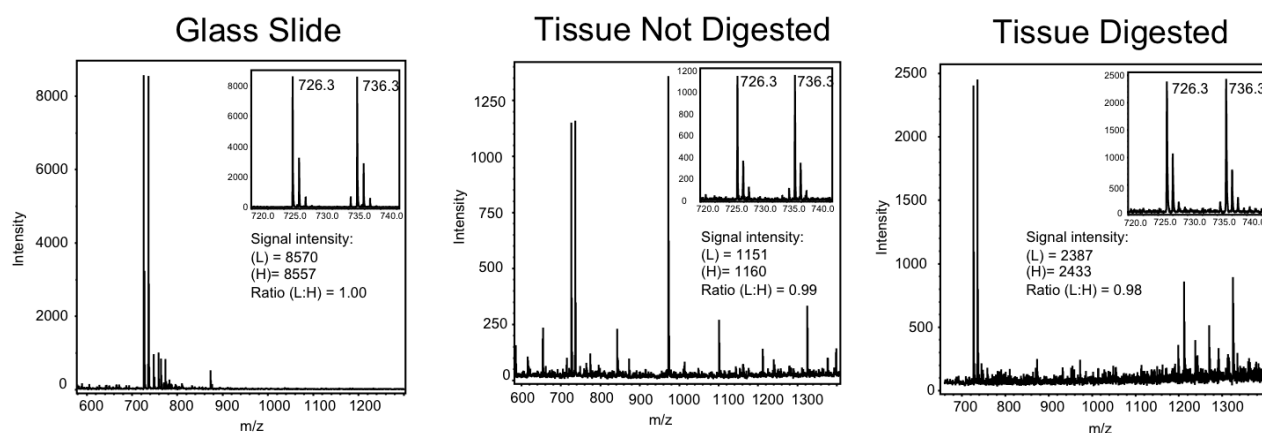


Figure 10. Ion Suppression Test.

A comparison between MBP ions on liver tissue (which does not contain MBP), and MBP ions on a glass slide in an ion suppression-free spot.

The light (m/z 726.3) and heavy MBP peptide (m/z 736.3) were spotted onto a glass slide, a section of liver tissue that was not digested with trypsin, and a section of liver tissue that was digested with trypsin. In each case, a 1:1 mixture of peptides was spotted, and the observed ratios for the three samples were very close to 1:1 (Figure 10).

Discussion

To demonstrate the proof-of-principle for a method that begins with protein identification and ends with the quantitation of the discovered protein, the following imaging experiments for the already well-characterized myelin basic proteins (MBPs) (Groseclose, et al., 2007) were performed. From the tissue section prepared and analyzed for protein detection, the ion images with m/z values of 14,097 and 18,351 are displayed along with a summed ion spectrum. Indeed, the predominant isoforms of MBP in adult rats are the 14 and 18.5 kDa isoforms.

On a 12 μm -thick slice of tissue from an adjacent portion of the brain, an in-situ protein digestion was performed to confirm the identify the 14 kDa and 18.5 kDa analytes based on the peptide molecular weights and sequences obtained from regions that displayed a similar spatial morphology. The trypsin solution is deposited onto the tissue by the aerosol generating Following the application of matrix, data acquisition (in the reflector positive ion mode with a spatial resolution of 125 μm and 200 shots per pixel) and image generation, ions were selected which displayed a similar distribution to the 14 kDa and 18.5 kDa target proteins (Figure 6). In this case, ion images are shown that correspond to m/z 726.5, m/z 1336.7, and m/z 1503.0 (Figure 7).

The MS/MS spectra acquired was uploaded to Mascot's MS/MS search engine for sequence identification (Perkins et al., 1997). The sequences of the three ions shown in Figure 7 were searched against the *Rattus norvegicus* database using BLASTp to

determine if they were unique within the rat proteome to the myelin basic protein isoforms (Altschul et al., 1990). One of the three MS/MS spectra acquired directly from the tissue following tryptic digestion and CHCA matrix coverage is shown in Figure 8, and the ion at m/z 726.5 was shown to have the amino acid sequence HGFLPR. All of these three ions were identified as tryptic peptides from myelin basic protein (Figure 9). These experiments confirm the results of a similar study (Groseclose et al., 2007) and demonstrate the feasibility of a bottom-up approach using MALDI imaging for protein identification.

The MALDI imaging technique for protein identification presents an alternative to the tissue homogenization based mass spectrometry techniques which are more time consuming and do not preserve spatial distribution of the analytes. To date, proteins identified by bottom-up MALDI imaging have been limited to only the most highly expressed proteins (Groseclose, et al., 2007; Schober et al., 2011). However, a major focus in the field of MALDI imaging is on the optimization and development of techniques to improve sensitivity and the analysis of lower abundance proteins. A technique already shown to improve sensitivity is the use of the triple quadrupole mass spectrometer over the more commonly-used TOF instrument (Prideaux et al., 2011).

The method described in this study uses a labelled peptide to quantify the amount of an endogenous tryptic peptide detected in a tissue section. It is important to demonstrate that these ions behave identically in the mass spectrometer under all conditions reported. To determine the homogeneity of the peptide mixture, and to look for any suppression

effects, I compared the ratios of the light to heavy (L:H) peptides on a glass slide to the ratio of the same solution spotted onto both digested and undigested tissue. Figure 10 shows that the ratio of the signal intensities for light (m/z 726.3) and heavy (m/z 736.3) peptide does not change with the different ion suppression conditions. Any suppression affects both isoforms equally, so ion suppression of the endogenous peptide is compensated for by the equal suppression of the Stable Isotope-labelled Standard SIS peptide. The recent paper by Leigh Anderson, et al. (2012) has also shown the reproducibility of MALDI when SIS peptides are used.

Chapter 3 - Quantitation of the Normalization Peptide.

Introduction

For an ion signal detected by MALDI imaging to be normalized using a reference standard, the standard must be homogeneously distributed over the tissue being analyzed. Normalization of the ion signal is an important step towards quantitation. Without normalization, intensity differences caused by the inhomogeneities in the matrix layer would lead to incorrect conclusions in the ion abundances.

The method proposed bases the quantitation of a protein from a tissue section on the ratio between a representative endogenous peptide and a homogeneously-deposited heavy version of the same peptide. As shown in Figure 5, a heavy peptide is deposited directly onto an ITO coated glass slide. The heavy peptide is then deposited onto a thin section of trypsin digested tissue. The amount of heavy peptide deposited needs to be determined in order for its use as a quantitative internal standard. Data acquisition for the quantitation of the sprayed heavy peptide method uses the Bruker ultraflex III TOF/TOF mass spectrometer.

Materials and Methods

Optimization of peptide deposition method

On coronal sections of rat brain which had previously been digested with trypsin (prepared using the method described in the previous chapter), a range of concentrations of heavy peptide were added to the ImagePrep reservoir, from 50 pmol/ μ l to 0.5 pmol/ μ l in 30% ACN/ 0.1% FA. The manual settings on the ImagePrep were also optimized. The best results came from a 2.0 pmol/ μ l concentration of the labelled peptide with the following ImagePrep settings: Cycles = 15, Power = 30%, Modulation = 0%, Time = 1 second, Incubation = 100 seconds, Dry = 100 seconds. The matrix (10 mg/mL CHCA/ 70% ACN/ 0.1% TFA) was applied with the following Imageprep settings: Cycles = 45, Power = 20%, Modulation = 10%, Time = 1 second, Incubation = 60 seconds, Dry = 100 seconds. The digested tissue sections coated in labelled peptide and CHCA matrix were analyzed on the Bruker ultraflex III in reflector mode. The results were displayed using the Bruker flexImaging software application.

Reproducibility of the aerosol deposition method

The light tryptic myelin peptide (m/z 726.5) was sprayed onto a blank ITO coated slide, followed immediately by the isotopically-labelled heavy version of the peptide (m/z 736.5) using the optimized spray method described above. Methanol was run through the ImagePrep between the spray applications to remove any residual peptide. Following the application of matrix, data was collected from a 1.6 cm x 1.7 cm portion of the slide by

MALDI-TOF MS in reflector positive mode. The results were displayed using the Bruker flexImaging software application.

MRM normalization

A coronal rat brain tissue section was prepared, digested, and covered in labelled peptide and CHCA matrix using the same methods and ImagePrep settings as described above.

The tissue section was analyzed using the Applied Biosystems QTRAP 4000. The spectra for the endogenous tryptic peptide and the heavy peptide were recorded in MRM mode using the transitions 726.5/ 324.2 and 736.5/ 324.2 respectively. The data was acquired using the Analyst and MSQ software applications and displayed using the custom-built imaging software for processing written in LabVIEW™ (National Instruments, Austin, TX). This software application automatically detects peaks within alignment traces which are placed on the sample substrate. The alignment traces allow the data to be unfolded into a 2-D image. Image contrast enhancement, dimensioning, and pixel-by-pixel analysis are all available within this custom software package. The application normalizes the data by dividing the signal from the light peptide by the signal from the heavy peptide.

Generation of Standard Curve

For the generation of the standard curve to determine the amount of labelled peptide sprayed per area, a series of dilutions of the synthesized unlabelled myelin basic protein tryptic peptide in a solution of 10 mg/ mL CHCA/ 70% ACN/ 0.1% TFA (0.05 pmol/μL, 0.1 pmol/μL, 0.2 pmol/μL, 0.4 pmol/μL, 0.6 pmol/μL, 0.8 pmol/μL and 1.0 pmol/μL)

were prepared from a 10 pmol/ μ L stock solution. A 0.5- μ L aliquot of each solution was spotted onto a glass slide that had been previously been sprayed with the heavy peptide. The labelled peptide was deposited onto the slide using the same spray method described above. The matrix spots were imaged using the Bruker ultraflex III in reflector mode with the laser set to 50 μ m in diameter. The spots were imaged with a 125 μ m x 125 μ m image resolution and an accumulation of 300 shots were summed per acquisition. The results were displayed using the Bruker flexImaging software application.

Reproducibility of Peptide/Matrix Spot Imaging

To determine the reproducibility of the calibration curve, five replicates of four concentrations of unlabelled peptide were spotted using the same method that was used to make the standard curve. Following the spray deposition of the heavy peptide, the slides were manually spotted with 0.5- μ L volumes of solutions containing 0.2 pmol/ μ L, 0.4 pmol/ μ L, 0.6 pmol/ μ L, and 0.8 pmol/ μ L of the light peptide in CHCA. The replicate spots were imaged using the Bruker ultraflex III in reflector mode with the laser set to 50 μ m in diameter, in a manner identical to the method for the imaging of the spots used in the calibration curve. The spots were imaged with a 125 μ m x 125 μ m image resolution and 300 shots were summed per acquisition. The results were displayed using the Bruker flexImaging software application.

Results

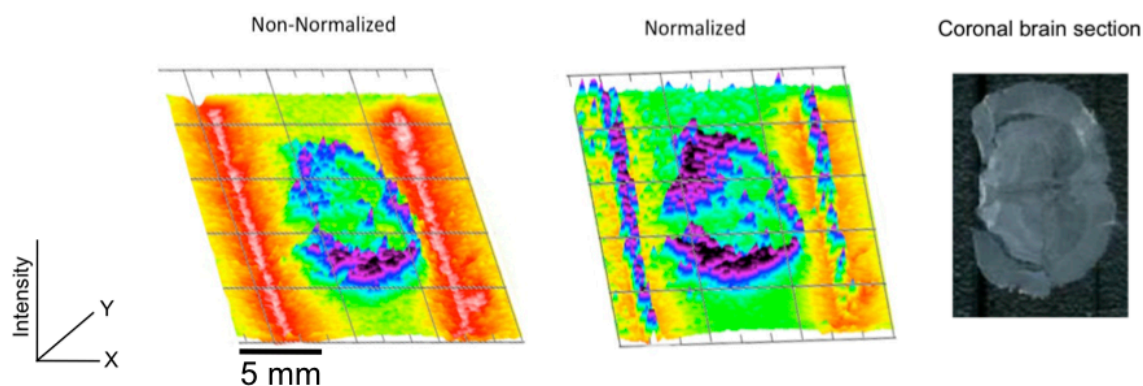


Figure 11. MALDI Images created from MRM data.

MALDI MRM images from a trypsin-digested coronal 10- μm thick section of rat brain. The digested tissue was sprayed with the heavy peptide and CHCA matrix. The two images on the left show the endogenous tryptic peptide (m/z 726.5) from myelin basic protein from a coronal section of rat brain tissue. The image in the middle has been normalized to the sprayed heavy peptide. The image on the right is the thin coronal section prior to trypsin digestion.

The image that was normalized to the externally-applied reference standard shows a more uniform expression pattern of the HGFLPR (m/z 726.5) endogenous tryptic MBP peptide.

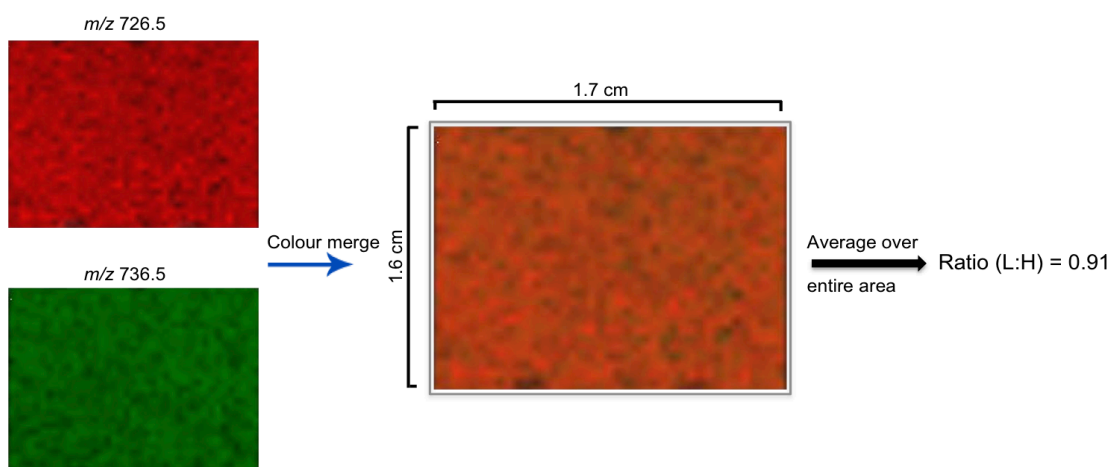


Figure 12. Reproducibility of the aerosol application of peptides.

The myelin basic protein tryptic peptide HGFLPR was synthesized with and without an isotopic label. A 2 pmol/ μ L solution of the heavy-labelled peptide was deposited onto a conductive ITO coated glass slide using the ImagePrep workstation in 15 one-second spray cycles. The same procedure was then followed for the subsequent application of the unlabelled peptide. The slide was then coated in CHCA matrix and an area 1.7 cm by 1.6 cm was analyzed on the MALDI TOF/TOF in reflector positive mode.

When solutions containing the same concentrations of light and heavy peptides are sequentially applied to the glass slide using the same manual settings on the ImagePrep station, the majority of the ratios between the signals of the peptides at each spot of ablation was 1:1. The average ratio over the entire area imaged was 0.91.

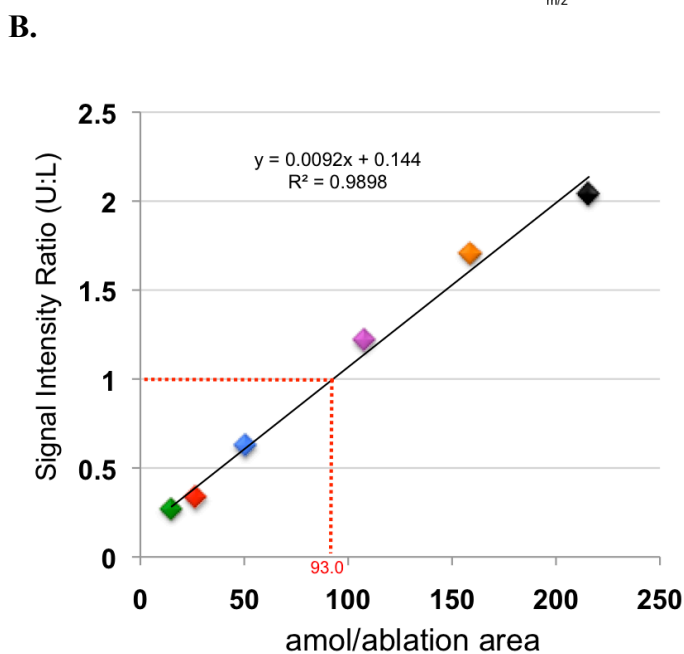
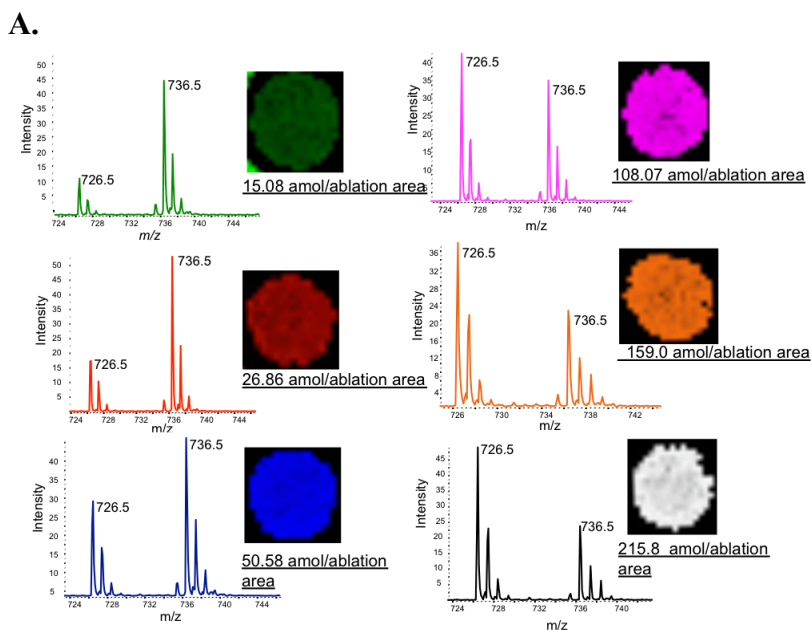


Figure 13. Absolute quantitation of heavy peptide by aerosol deposition.

Following the application of the heavy peptide, 0.5 μL of the synthesized light version of the m/z 726.5 myelin peptide was spotted onto a conductive ITO coated glass slide in increasing concentrations. **A.** Ion images of the spots obtained with a 125- μm spatial resolution inset into a zoomed in region of the total ion chromatogram. Six different concentrations of the light peptide were spotted onto the slide. Each pixel is the sum of 300 shots, and there were approximately 250-300 pixels per spot image. **B.** The total area of each spot was calculated in order to determine the amount of heavy peptide per ablation area, this was then plotted

against the ion signal intensity ratio of the light to heavy peptide to generate a standard curve.

The external calibration curve has a coefficient of determination (R^2) of 0.9898. The amount of heavy labelled peptide deposited by the ImagePrep during the application was determined to be 93.0 amol/ ablation area. The laser diameter is 50 μm ; therefore the ablation area represents 1963.5 μm^2 on the slide.

Spot Concentration (L) (pmol/ μl)	0.2	0.4	0.6	0.8
(L:H) signal ratio multiplied by the spot area (μm^2).	2.96 E06	3.25E06	3.98E06	4.19E06
	2.91 E06	3.35E06	3.55E06	4.92E06
	2.53E06	3.18E06	3.29E06	4.55E06
	2.49 E06	3.60E06	3.02E06	4.23E06
	2.54E06	3.54E06	3.15E06	4.64E06
%CV	8.56	5.409	11.23	7.50

Table 1. Reproducibility of the spot imaging method for generation of the calibration curve.

Amount of labelled peptide per area (amol/ablation area)	Coefficient of determination (R^2)
43.7	0.97775
93.0	0.98980
100.0	0.97385

Table 2. Results from the generation of three separate standard curves over a one-month period. Each ablation area represents 1963.5 μm^2 of the slide.

Testing the reproducibility of the spot imaging method showed that CVs of less than 12% could be obtained within an experimentally-determined region of the slide where the spray is uniform. Spots with larger areas will give lower L:H ratios. To compensate for the differences in spot areas, the sum of the spectra from the 300 shots was multiplied by

the spot area. After imaging the spots the area of each spot and the ratio of the signals for the heavy and light peptide over the entire area of each spot were determined. This signal ratio (L:H) was then multiplied by the area of the spot which normalized the data.

Discussion

A 10 μm -thick coronal section of trypsin-digested rat brain tissue was coated in the labelled MBP peptide and matrix using the method described above. The peptide was applied over the tissue in a homogenous layer; thus, it can be used to normalize the endogenous signal. Figure 11 displays the importance of normalization for MALDI-MRM imaging. The symmetrical nature of the brain provides an internal control for the imaging process. The image on the left, which has not been normalized to the labelled peptide, shows less bilateral symmetry in the expression pattern and signal intensity of the endogenous tryptic MBP peptide compared to the normalized image on the right. The externally-applied reference standard has reduced the matrix localization effects, as well as any compound specific ion suppression due to the heterogeneity of the brain tissue.

Because the endogenous peptide was normalized to a uniformly deposited stable isotope-labelled peptide analog, the ratio of these two signals can be used to calculate the actual quantity of the MBP isoforms present. The amount of labelled peptide that is sprayed onto the tissue must be known in order to perform this calculation, however.

The external quantitation method is based on the known quantity of labelled peptide per area on the blank glass slide and extrapolating this quantity to the area of the tissue. For

this assumption to be valid, it must be proven that the Bruker ImagePrep station is capable of reproducible spray applications. Figure 12 shows two sequential spray applications of the peptides onto a blank glass slide. The light tryptic MBP peptide (m/z 726.5) was sprayed, followed by the isotopically-labelled heavy version of the same peptide (m/z 736.5) using the same spray settings. Following the application of matrix, data was collected from a portion of the slide by MALDI-TOF MS in reflector positive mode. The larger rectangle in the centre is a color-merge of light (red) and the heavy (green) ion signals. In the centre rectangle, the most intense green colour comes from parts of the slide where there was an excess of light peptide. Likewise, the most intense red colour comes from the parts of the slide where there was an excess of heavy peptide. The orange spectrum colour is representative of areas where the peak areas were close to a one-to-one ratio. Although the uniformity is not perfect, signal intensities of close to 1:1 were observed for the majority of the spectra acquired. This demonstrates that the spray deposition is quite reproducible when the isotopically-labelled standards are applied in to the blank slide and the tissue section in succession. This region, however, could possibly be different with different sprayers or spotters, and this area of homogeneity should therefore be determined for each device. The overall results are good, but my hypothesis is that it should be possible to get peak area ratios that are even closer to 1:1, and an even more homogenous distribution, by increasing the number of spray cycles and using a less-concentrated peptide solution. This is something to examine in future experiments.

The method described in Figure 5A was applied to a blank portion of an ITO coated glass slide. Increasing concentrations of the synthetic unlabelled peptide in matrix were

spotted onto the slide and imaged by MALDI-TOF MS in the reflector mode. The images of these spots and their corresponding ion signal spectra are shown in Figure 13A. The ratios between the signal intensities of the light (m/z 726.5) and heavy (m/z 736.5) peptides were averaged over the entire area of these spot and plotted against the amount of light peptide per ablation area to generate the standard curve shown in Figure 13B. The TOF instrument has a nominal ablation spot diameter of 50 μm , therefore, each ablation area represents 1963.5 μm^2 . An independent set of experiments that tested the reproducibility in individual spots such as those used to generate the standard curve obtained CV values of less than 12% (Table 1).

Using the equation from the regression line that was determined from the standards, the amount of labelled peptide per area deposited by aerosol deposition was calculated to be 93.0 amol/ ablation area. Although the reproducibility of the Bruker Imageprep station for sequential peptide applications is demonstrated, the extent of the variability of the spray application over time is evident from the results displayed in Table 2. Three standard curves were made over a one-month period. The spray settings and slide positioning in the ImagePrep station were kept constant in all three experiments. This method consistently produces a linear calibration curve, as shown by the R^2 values in Table 2, even though the quantity of peptide sprayed varied over extended periods of time. This demonstrates the necessity for a standard curve to be generated along with each MALDI-MRM imaging experiment when quantitation is desired.

Chapter 4 - Quantitation of the Myelin Basic Protein Isoforms on a Rat Brain Tissue Section.

Introduction

The quantitation of peptides as molecular surrogates for their precursor proteins is the most common MS-based protein quantitation method. This commonly-used method is more challenging when the proteolytic digestion must take place on-tissue. It is complicated by the requirement that the localization of the proteolytic peptides must match the original location of the precursor proteins; therefore, diffusion across the tissue must be prevented. The ImagePrep deposits very small droplets onto the tissue in a controlled environment, making it well-suited for on-tissue proteolytic digestion.

MALDI imaging experiments generally do not show ion signals for proteins greater than 25 kDa (van Remoortere et al., 2010). Tryptic digestion of these proteins results in peptides that are within a mass range that is accessible by MALDI imaging. However, the initial complexity of the tissue sample increases dramatically upon proteolytic cleavage; furthermore, the resulting peptides typically fall within the same mass range (m/z 800 – 3000) (Kuster et al., 2005). This means that signals from individual peptide signals can be lost due to signal overlap in traditional TOF/TOF MALDI imaging. The increased selectivity of a MALDI-QTRAP using the MRM mode can help resolve overlapping signals from isobaric ions that might be present in the complex mixture resulting from a tissue digest.

Materials and Methods

Efficiency of Trypsin Digest

Each of three ITO coated glass slides was fixed with a 10 μm coronal section of rat brain. The slides were rinsed in a series of alcohol and water solutions -- 1 x 15 seconds in 70% ethanol and 1 x 15 seconds in 90% ethanol : 9% acetic acid (v/v). One slide was coated directly with 10 mg/mL CHCA in 70% ACN/ 0.1% TFA using the following ImagePrep setting in manual mode: cycles = 45, power = 20, modulation = 10, spray = 1s, incubation = 60s, and dry = 100s. On the second slide, the tissue was digested with trypsin using the same method previously described: The trypsin was diluted with 100 mM Ammonium bicarbonate to a final trypsin concentration of 46 $\mu\text{g}/\text{mL}$. The trypsin was applied to the tissue using the Bruker ImagePrep station in manual mode using the following optimized settings: cycles = 30, power = 20, modulation = 10, spray = 1s, incubation = 60s, and dry = 100s. Following the digestion, CHCA was applied to the section using the same ImagePrep settings described for the previous slide. The third section was coated with 100 mM ammonium bicarbonate using the same ImagePrep settings used for the trypsin digest, and then coated in CHCA using the same method as the previous two slides. The three tissue sections were analyzed in reflector mode using the Bruker ultraflex III on a portion of the tissue where myelin basic protein (MBP) is expressed.

Quantitation of MBP using MALDI-MRM imaging

Following the deposition of the heavy peptide onto a blank ITO coated glass slide, a coronal rat brain tissue section was prepared, digested, and covered in labelled peptide

and CHCA matrix using the same methods and ImagePrep settings as described above. The tissue section was analyzed using the Applied Biosystems QTRAP 4000. The spectra for the endogenous tryptic peptide and the labelled peptide were recorded in MRM mode using the transitions 726.5/ 324.2 and 736.5/ 324.2, respectively. The transition 358.3/342.2 from pen markings flanking the tissue section was used to align the data, and the transition 700.0/400.0 was used to zero the instrument between detection of the peptides. The data was acquired using Analyst and MSQ software and was displayed using custom-built imaging software for processing which was written in LabVIEW (National Instruments, Austin, TX).

Results

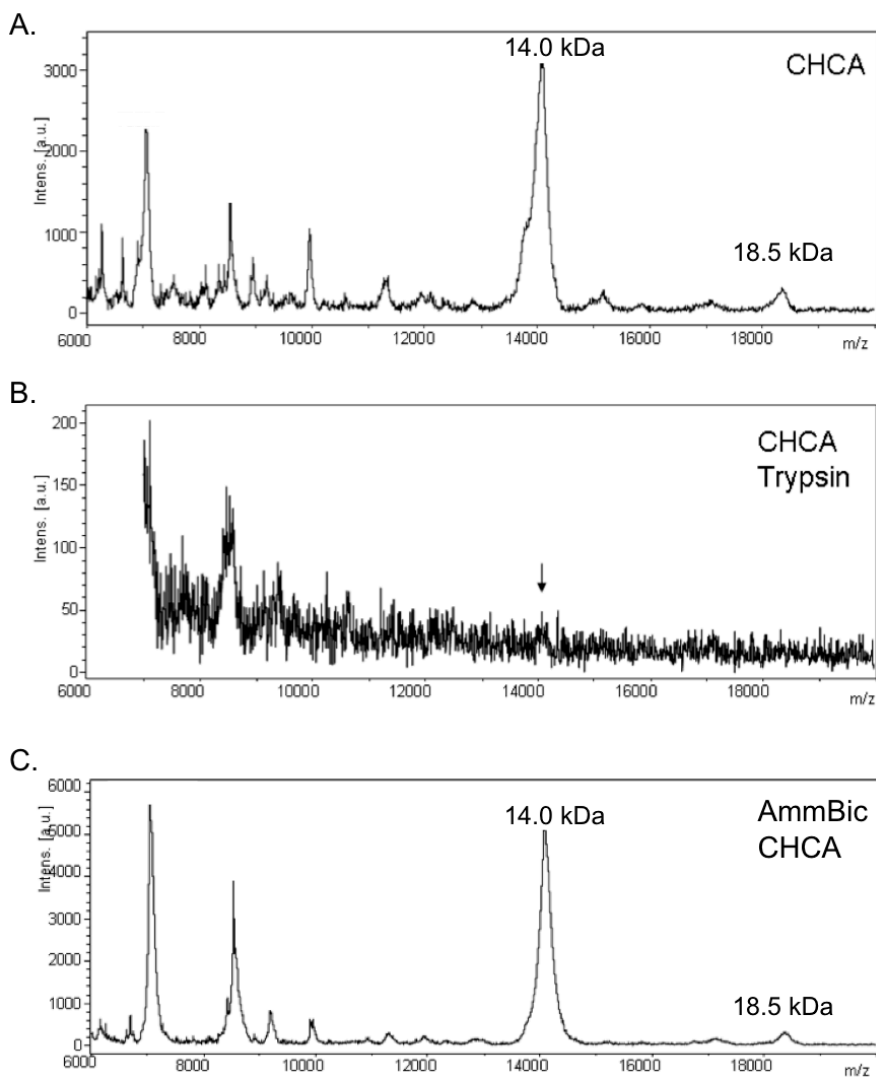


Figure 14. Efficiency of trypsin digestion.

A. A summed ion spectrum analyzed in linear positive mode, using CHCA as the matrix. B.

A summed ion spectrum that was obtained from a section following an in situ trypsin digestion and subsequent application of CHCA matrix using the Bruker ImagePrep station.

C. A summed ion spectrum that was obtained from a section following the application of 100 mM ammonium bicarbonate and subsequent application of CHCA matrix using the Bruker ImagePrep station. The data was obtained from an analysis in the linear positive mode on a portion of the tissue where myelin basic protein (14.0 kDa and 18.5 kDa) expression was observed.

The ion signals corresponding to the intact MBP isoforms (14 kDa and 18.5 kDa) that are observed in the non-digested tissue sample (Figure 14A) are greatly reduced in the trypsin-digested tissue (Figure 14B). Note the change in scale of the Intensity axis. The signals for the intact MBP isoforms are not reduced in the tissue that has only been sprayed with 100 mM ammonium bicarbonate (Figure 14C) and the spectrum is quite similar to those acquired with SA and CHCA alone (Figure 14A).

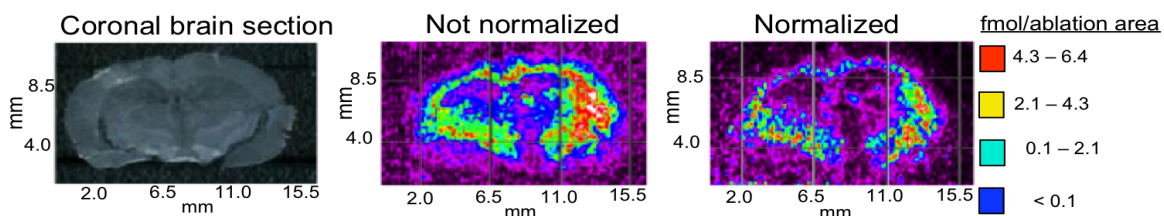


Figure 15. *MALDI Images created from MRM data.*

The image shows the concentration and distribution of the endogenous tryptic peptide from myelin basic protein from a coronal section of rat brain tissue. The data used to generate these images was acquired on the MALDI-QTRAP in MRM mode.

The image on the right in Figure 15 is normalized to the sprayed labelled peptide that had been determined to be distributed on the tissue at $93.0 \text{ amol}/1963.5 \text{ } \mu\text{m}^2$ (see Figure 13). Based on the MRM data acquired, the amount of endogenous peptide per area was calculated from the ratio of the endogenous to the labelled peptides which was then multiplied by $426.3 \text{ amol}/\text{ablation area}$.

Discussion

For quantitation based on stable-isotope-labelled peptides, the protein must be converted to peptides and the quantity of the peptides must accurately reflect the amount of protein in the tissue. It is therefore desirable to achieve as complete a digestion as possible of the proteins of interest in the tissue. Digestion methods have been shown to be quite reproducible if the digestion conditions are maintained (Proc et al., 2010). Figure 14 shows that following the digestion step, the intact protein is barely detectable, which is evidence of a high degree of digestion, however, more experiments are needed in order to verify complete digestion.

The selectivity of the MRM method greatly increases the sensitivity due to the removal of background ions by the first quadrupole. The MRM ion pairs used to acquire the data needed to construct the image shown in Figure 15 were m/z 726.5/ 324.2 and 736.5/324.2, which have the peptide sequence HGFLPR. The m/z 726.5/ 324.2 transition represents the endogenous tryptic peptide of the MBP isoforms from the *in situ* digestion, and the m/z 736.5/324.2 transition represents the labelled peptide that was used as an external standard. The m/z 324.2 fragment is likely to be the result of a dehydration of the b3 ion. The 324.3 fragment is also seen in the MS/MS spectrum of the HGFLRP peptide analyzed on the TOF/TOF instrument (Figure 8). The signal for the dehydrated b3 fragment was significantly stronger than the signal for the b3 fragment when the quadrupole instrument was utilized. The b3 ion (HGF) has m/z of 342.2, which is an 18 Da difference from the m/z 324.2 used for the transition. A shift of 18 Da is characteristic for the loss of a water molecule. Dehydration of a singly charged glycine-

containing peptide during CAD fragmentation occurs through retro-Koch and retro-Ritter type reactions (Reid et al., 1998).

The image on the right has been normalized to the sprayed standard peptide. Because the ratio of the endogenous and the SIS peptide is used for quantitation, the externally-applied reference standard compensates for any non-homogeneity in the matrix application, as well as any differences in ion suppression due to the heterogeneity of the tissue. This results in the correct symmetrical distribution observed in the image on the right side of Figure 15, as compared to the asymmetrical distribution obtained from the un-normalized data (Figure 15, center).

This method is also capable of displaying the amount of endogenous peptide at any location within the tissue by clicking on the image generated by the software. The amount of peptide is determined differently when using the MALDI-quadrupole mass spectrometer compared to the MALDI-time-of-flight mass spectrometer. With the TOF instrument, the laser rasters across the tissue in discrete spots. As described above, the laser in the MALDI source attached to the MALDI-quadrupole fires continuously while moving in a serpentine pattern over the tissue. In this experiment the dwell time was 50 ms and the laser moved across the tissue with a velocity of $0.9 \mu\text{m}$ per millisecond, therefore each ablation area for this method represents the volume of peptides volatilized by the laser as it travels across $45 \mu\text{m}$ of a $10 \mu\text{m}$ -thick tissue section. The diameter of the laser is $200 \mu\text{m}$ and it traverses $45 \mu\text{m}$ of tissue during each dwell time, giving an ablation area of $9000 \mu\text{m}^2$. The spatial incrimination in the y dimension was $100 \mu\text{m}$.

Based on the MRM data acquired, the amount of endogenous peptide per area was calculated from the ratio of the endogenous to the labelled peptides and then multiplied by 426.3 amol/ablation area. It is important to note that the quantities of protein determined by this method come from tissue sections that were 10 μm thick, and therefore need to be considered in three dimensions.

As in other methods that use peptides as surrogates for proteins, this imaging method quantifies peptide signals resulting from a tryptic digestion step, therefore, if any modified forms of the parent protein are present, this information may be lost. For example, figure 6 shows two isoforms of MBP (14 kDa and 18.5 kDa), as identified by Crecelius, et al., (2005) in mouse brain. Because the peptides used in these calculations come from the portions of these highly-homologous protein isoforms that are identical, the amount of peptide calculated from the MRM MALDI data corresponds to the tissue concentrations of the *sum* of the protein isoforms that contain these peptides. However, if it were desirable to quantitate a *specific* isoform, this limitation can be overcome by using a peptide that is unique to the isoform and is detectable by MALDI (Zulak et al., 2009).

This study represents the first on-tissue absolute quantitation of MBP, therefore, a comparison of the results with another method is not possible. However, we can calculate the average MBP quantity per μm^3 from a whole brain and compare this to our results. Using data from a study on MBP in mouse brain (Barbarese et al., 1972), we calculated the amount of MBP protein in mouse brain to be 0.045 amol/ μm^3 . From the data collected in our study we determined the quantity of MBP per μm^3 to be in a range

between 0.001 - 0.071 amol/ μm^3 . While MBP is one of the most abundant proteins in brain tissue, it is not expressed homogeneously throughout the brain, therefore, an average calculated for the entire brain is only an estimate. Furthermore, the results from my study are from rat brain tissue, which could be slightly different of brain tissue from mice.

The strategy employed here is a targeted imaging approach, it is not a non-targeted strategy like traditional MALDI imaging methods, but the goal here is to determine tissue-*concentrations*, not simply to determine relative signal intensities. Furthermore, as is the case for classical in-solution MRM quantitative assays, this method also requires that each peptide used in the quantitation protocol be synthesized in its labelled and unlabelled form.

Currently our instrument is limited to 5 transitions. This experiment used 1 transition for the endogenous peptide, 1 transition for the SIS, 1 transition to blank the instrument, and 1 transition for the alignment. Thus, this method demonstrated the quantification of one peptide per tissue slice; although another SIS peptide could be added to the method for the quantification of two peptides per slice. In these proof-of-concept experiments, I chose to use one peptide from MBP instead of two because the initial focus was on method development and the feasibility of the approach. Future experiments should use at least two peptides per protein (with one transition per peptide) for a more confident quantitative result (Domanski et al., 2012).

Chapter 5 - Future work

Introduction

Alternative reagent deposition technologies can deposit trypsin, matrix, and other liquids onto tissue sections in discrete spots using very small volumes (80 -150 pL) (Végvári et al., 2010) either using technology similar to that used in inkjet printers (Nokihara et al., 2002), or by the ejection of droplets from a fluid interface in a reservoir by acoustic energy (Baluya et al., 2007; Aerni et al., 2006). While the application of solutions using spotting technologies is more controlled and homogenous, the distance between sample spots is larger than when sprayed droplet deposition is used. The minimum centre-to-centre distance between matrix spots deposited by a spotter is 200 μm using SA, and 150 μm using CHCA. This limits the achievable image resolution (Végvári et al., 2010). However, if image resolution below these limits is not necessary, then the spotting method has the potential to be a very valuable tool for quantitative MALDI imaging.

The Portrait 630TM spotter by Labcyte is a fully-automated acoustic droplet ejection system that deposits reagents like MALDI matrix onto tissue sections. The fluid is ejected in small droplets from open wells by focusing ultrasonic acoustic energy at the meniscus of the fluid sample. A transducer transmits sound waves through the bottom of the reservoir and through the fluid. An upwelling is created at the fluid surface by the pressure of the focused acoustic waves, resulting in the droplet flying vertically upwards toward the tissue section that is suspended above the ejection reservoir. The ejected volume is a constant 150 pL. Because the system is nozzle free, the amount of liquid that

is applied at the beginning of the method is same amount at the end. Spotting systems that use a piezo nozzle, such as the ink jet systems, have problems with clogging. This would be especially problematic for the homogenous application of standards and matrix (Aerni et al., 2006). The Portrait 630 spotter accommodates a wide range of reagent types and can apply cycles of one droplet per spot in less than two minutes with a user-adjustable droplet deposition rate of up to 200 droplets/second. It allows drop-on-drop applications for enzyme digest followed by MALDI matrix and a selective specification of the target area that is not possible with the spray methods. The Labcyte acoustic spotter is ideal for quantitative MALDI imaging because it is nozzle-free, reproducible and precise.

Methods and Materials

Overlay of light and heavy peptides

The light and heavy peptides were diluted separately in 10 mg/mL CHCA/ 70% ACN/ 0.1% TFA to a concentration of 0.5 pmol/ μ l. The light peptide was spotted by the labcyte Portrait 630 spotter (Sunnyvale, California) in 15 iterations with 1.5 mins between each iteration to allow drying. The heavy peptide then loaded and spotted directly over top of the light peptide using the same method. The method was set using four blocks with a 600 μ m pitch to form a final pitch of 300 μ m. The slide was stored at -20°C until it was shipped in dry ice from Sunnyvale, California to Victoria, British Columbia. The slide was put under vacuum to allow it to equilibrate to room temperature for 20 mins. The slide was imaged using the Bruker ultraflex III in reflector mode with

an image resolution of 75 μm . The software used for data acquisition and analysis was flexControl, and flexImaging.

Image of Endogenous MBP peptide.

A 10 μm coronal section of flash frozen rat brain tissue was heat fixed to an ITO coated glass slide. The slide was placed in a vacuum for 60 min to allow the tissue section to dry and equilibrate to room temperature. The slide was rinsed in a series of alcohol and water solutions -- 1 x 15 seconds in 70% ethanol and 1 x 15 seconds in 90% ethanol : 9% acetic acid (v/v). The slide was shipped to Sunnyvale, California from Victoria, British Columbia on dry ice and then stored at -20°C until use. Using the Portrait 630 spotter, the tissue was digested with 90 $\mu\text{g}/\text{mL}$ of trypsin using a 15 iteration method with 1.5 mins between each iteration, and then left overnight. The following morning, 0.5 pmol/ μl of the heavy peptide in 10 mg/mL CHCA/ 70% ACN/ 0.1% TFA matrix was spotted over the trypsin spots in 15 iterations with 1 min between each iteration. The slide was shipped back to Victoria, British Columbia on dry ice. The slide was placed in a vacuum for 60 min to allow the tissue section to dry and equilibrate to room temperature before imaging on the Bruker ultraflex III Bruker ultraflex III in reflector mode with an image resolution of 75 μm . The software used for data acquisition and analysis was flexControl, and flexImaging.

Results

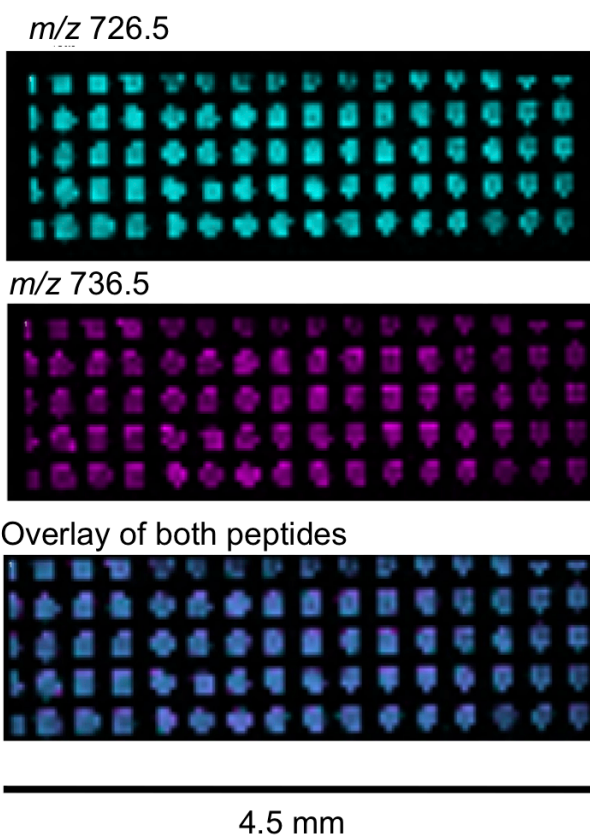


Figure 16. MALDI TOF images of the heavy and light peptides overlaid using the Labcyte Portrait 630 spotter.

MALDI TOF images of the spots from the application of the light (upper) and heavy (middle) peptides in matrix. The bottom image shows the overlay of the resulting images.

The Portrait 630 spotter applied the heavy peptide over top of the light peptide with only a minor spatial shift (less than 20 μm).

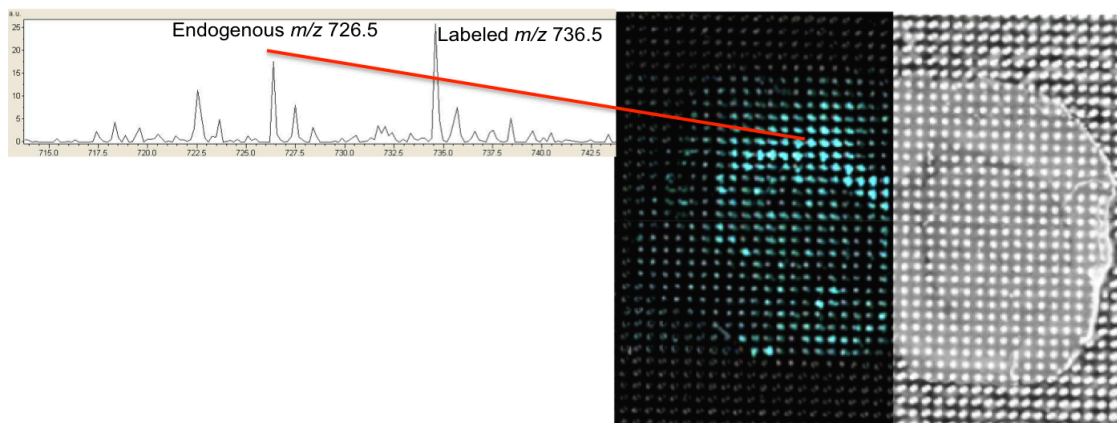


Figure 17. MALDI TOF image of endogenous tryptic MBP peptide and summed spectra. Coronal rat brain section with trypsin and heavy peptide/matrix applied using the Portrait 630 spotter. Image was acquired on a MALDI-TOF in reflector mode.

The signal for the endogenous peptide (m/z 726.5) was observed in the spectra for several pixels in the resulting MALDI TOF image. The pattern of the pixels representing the endogenous MBP tryptic peptide (Figure 17) partially follows the morphology observed in figures 6 and 7.

Discussion

The capability of directly overlapping spots of liquid is important for a spotting technology to be used for quantitative MALDI imaging. For the amount of heavy peptide to represent the amount of a protein in the tissue, it must be applied directly on top of the portions of the tissue that have been proteolytically digested. The Portrait 630™ spotter by Labcyte is capable of sequential applications of a liquid that overlaps the previous application, as demonstrated by Figure 16. I have shown the successive application of a synthetic peptide/matrix deposited on top of another synthetic peptide/matrix that was applied using the same settings and method. The overlap of successive applications of

trypsin and the heavy peptide is demonstrated in figure 17. The signal from the endogenous peptide, as demonstrated by the MALDI image, does not form uniform spots, suggesting that the trypsin-containing spots spread over the tissue. The method used to apply the trypsin needs to be optimized to minimize amount of this spreading. However, while the experiment shown in Figure 17 was not successful in demonstrating that this technology is capable of overlaying applications of trypsin and the heavy peptide, it does confirm that proteolytic digestion of proteins using acoustic spotting is feasible (Groseclose et al., 2007).

A platform of quantitative MALDI imaging using acoustic spotting technology could possibly eliminate much of the variability caused by the aerosol deposition method. This type of spotter can reproducibly apply a known quantity of the heavy peptide to the tissue every 300 μm . This could eliminate the need for an external calibration curve.

Chapter 6 - Conclusions

This study demonstrated that homogenous deposition of the stable-isotope-labelled internal standard is achievable with an aerosol spraying system. Because the endogenous and SIS peptides have the same physicochemical properties, and the ratio of these two ion signals is used for quantitation, the presence of this internal standard in each MALDI MS scan allows the accurate quantitation of the target tissue protein over two orders of magnitude in concentration, while maintaining the spatial localization information on the protein in the tissues. Thus, the results in this study have validated our hypothesis that quantitative MALDI Imaging, based on MRM with stable-isotope-labelled peptides, can be successfully performed on tissue slices. We have demonstrated that accurate tissue concentrations can be determined from these quantitative MALDI imaging experiments, and that this technique has the potential for being used to determine disease-related protein biomarkers in tissue slices. Further experiments, such as alternative spotting/deposition techniques, including acoustic spotting, should be performed in order to refine this technique. These deposition techniques could possibly eliminate the need for an external calibration curve.

Bibliography

- Aerni, H.-R.; Cornett, D. S.; Caprioli, R. M. *Analytical Chemistry* **2006**, *78*, 827-834.
- Akiyama, K., Ichinose, S., Omori, A., Sakurai, Y. and Asou, H. *Journal of Neuroscience Research*, **2002** *68*: 19–28.
- Alfassi, Z. B. *Journal of the American Society for Mass Spectrometry* **2004**, *15*, 385–387.
- Altschul, S. F.; Gish, W.; Miller, W.; Myers, E. W.; Lipman, D. J. *Journal of Molecular Biology* **1990**, *215*, 403-410.
- Anderson, L.; Razavi, M.; Pearson, T.; Kruppa, G.; Paape, R.; Suckau D.; *Journal of Proteome Research* **2012**, *11*, 1868-78, DOI: 10.1021/pr201092v
- Baluya, D. L.; Garrett, T. J.; Yost, R. A. *Analytical Chemistry* **2007**, *79*, 6862–6867.
- Barbarese, E.; Carson, J. H.; Braun, P. E. *Journal of Neurochemistry* **1972**, *31*, 779-782.
- Campagnoni, A.; Campagnoni, C.; *In Myelin biology and disorders.*; Lazzarini, R. A., Griffin, J. W., Lassman, H., Nave, K.-A., Miller, R. H., Trapp, B. D., Eds.; Elsevier Academic Press: San Diego, 2004, pp 387–400.
- Caprioli, R. M.; Farmer, T. B.; Gile, J. *Analytical Chemistry* **1997**, *69*, 4751-4760.
- Castellino S.; Groseclose R. M.; Wagner D.; *Bioanalysis* **2011**, *3*(21), 2427-2441
- Chaurand, P.; Sanders, M. E.; Jensen, R. A.; Caprioli, R. M. *American Journal of Pathology* **2004**, *165*, 1057-1068.
- Chughtai K, Heeren RM. *Chemical Reviews*. **2010**, 110(5):3237-77
- Clemis E J, Smith D S, Camenzind A G, Danell R M, Parker C E, Borchers C H. *Anal Chem*. **2012** ;84(8):3514-22..
- Crecelius, A. C.; Cornett, D. S.; Caprioli, R. M.; Williams, B.; Dawant, B. M.; Bodenheimer, B. *Journal of the American Society for Mass Spectrometry* **2005**, *16*, 1093-1099.
- Cui W, Rohrs HW, Gross ML. *Analyst*. **2011**, 136(19):3854-64.

- Domanski, D.; Percy, A. J.; Yang, J.; Chambers, A. G.; Hill, J. S.; Cohen Freue, G. V.; Borchers, C. H. *Proteomics, in press* **2012**.
- Duncan, M. W.; Roder, H.; Hunsucker, S. W. *Briefings in Functional Genomics and Proteomics* **2008**, *7*, 355-370.
- Gross, J. H.; Mass Spectrometry: A textbook. **2004**, Springer
- Groseclose, M. R.; Andersson, M.; Hardesty, W. M.; Caprioli, R. M. *Journal of Mass Spectrometry* **2007**, *42*, 254-262.
- Jiang J.; Fuller, J.; Kawula, T.; Borchers, C.; *Analytica Chimica Acta*. **2007**, *605*(1): 70-79.
- Kaletaş, B. K.; van der Wiel, I. M.; Stauber, J.; Lennard, J. D.; Güzel, C.; Kros, J. M.; Luider, T. M.; Heeren, R. M. *Proteomics* **2009**, *9*, 2622-2633.
- Kamholz, J.; Toffenetti, J.; Lazzarini, R. A. *Journal of Neuroscience Research* **1988**, *21*, 62-70.
- Karas M.; Gluckman M.; Schafer, J.; *J. Mass Spectrom.* **2000**, *35*, 1-12
- Kondrat, R. W.; McClusky, G. A.; Cooks, R. G.; *Anal Chem* **1978**, *50*(14), 2017-2021.
- Kuster B, Schirle M, Mallick P, Aebersold R. *Nature Reviews. Molecular Cell Biology*. **2005**, *7*:577-83
- Kuzyk, M. A.; Parker, C. E.; Borchers, C. H. In *Methods in Molecular Biology*; Backvall, H., Ed.; Humana Press, 2011, in press.
- Kuzyk, M. A.; Smith, D.; Yang, J.; Cross, T. J.; Jackson, A. M.; Hardie, D. B.; Anderson, N. L.; Borchers, C. H. *Molecular and Cellular Proteomics* **2009**, *8*, 1860-1877.
- Meistermann, H.; Norris, J. L.; Aerni, H.-R.; Cornett, D. S.; Friedlein, A.; Erskine, A. R.; Augustin, A.; De Vera Mudry, M. C.; Ruepp, S.; Suter, L.; Langen, H.; Caprioli, R. M.; Ducret, A. *Molecular and Cellular Proteomics* **2006**, *5*, 1876-1886.
- Nokihara, K.; Mihara, H. *Tanpakushitsu Kakusan Koso* **2002**, *47*, 626-632.
- Ong, S.; Mann, M. *Nature Chemical Biology* **2005**, *1*, 252 – 262.
- Perkins, D.; Pappin, D.; Creasy, D.; Cottrell, J. *Electrophoresis* **1999**, *18*, 3551-3567
- Prideaux, B.; Dartois, V.; Staab, D.; Weiner, D. M.; Goh, A.; Via, L. E.; Barry, C. E.; Stoekli, M. *Analytical Chemistry* **2011**, *83*, 2112-2118.

- Proc, J. L.; Kuzyk, M. A.; Hardie, D. B.; Yang, J.; Smith, D. S.; Jackson, A. M.; Parker, C. E.; Borchers, C. H. *Journal of Proteome Research* **2010**, *9*, 5422-5437.
- Rasmussen, G. T.; Isenhour, T. L. *Journal of Chemical Information and Computer Sciences* **1979**, *19*, 179-186.
- Ried, G. E.; Simpson, R. J.; *J Am Mass Spectrom.* **1998**, *9*: 945-956
- van Remoortere A, van Zeijl RJ, van den Oever N, Franck J, Longuespée R, Wisztorski M, Salzet M, Deelder AM, Fournier I, McDonnell LA. *Journal of the American Society for Mass Spectrometry.* **2010**, *11*:1922-9.
- Reyzer, M. L.; Hsieh, Y.; Ng, K.; Korfmacher, W. A.; Caprioli, R. M. *Journal of Mass Spectrometry* **2003**, *38*, 1081-1092.
- Roepstorff, P, and J Fohlman. *Biomedical Mass Spectrometry* *11* (1984): 601.
- Roth, H. J.; Kronquist, K. E.; Kerlero de Rosbo, N.; Crandall, B. F.; Campagnoni, A. T. *Journal of Neuroscience Research* **1987**, *17*, 321-328.
- Sanchez JC, Corthals GL, Hochstrasser DF. *Biomedical Applications of Proteomics*. Wiley-vch Verlag; Gmbh Weinheim: **2004**. p. 373.
- Seeley, E. H.; Oppenheimer, S. R.; Chaurand, P.; Caprioli, R. M.; *J Am Mass Spectrom.* **2008**, *19*(8), 1069-77.
- Schober, Y.; Schramm, T.; Spengler, B.; Römpf, A.; *Rapid Communications in Mass Spectrometry.* **2011**, *25*, 2475–2483
- Troendle, F. J.; Reddick, C. D.; Yost, R. A. *Journal of the American Society for Mass Spectrometry* **1999**, *10*, 1315-1321.
- Végvári, A.; Fehniger, T. E.; Gustavsson, L.; Nilsson, A.; Andrén, P.; Kenne, K.; Nilsson, J.; Laurell, T.; Marko-Varga, G. *Journal of Proteomics* **2010**, *73*, 1270-1278.
- Zulak, K. G.; Lippert, D. N.; Kuzyk, M. A.; Domanski, D.; Chou, T.; Borchers, C. H.; Bohlmann, J. *The Plant Journal* **2009**, *60*, 1015–1030.